*J. Fluid Mech.* (1982), *vol.* 115, *pp.* 187-216
*Printed in Great Britain*



# The creeping motion of liquid drops through a circular tube of comparable diameter: the effect of density differences between the fluids

By W. L. OLBRICHT† AND L. G. LEAL
Department of Chemical Engineering, California Institute of Technology, Pasadena

(Received 2 June 1980 and in revised form 19 May 1981)

Results of experiments on the low-Reynolds-number flow of non-neutrally buoyant drops through a straight circular tube are reported. The undeformed radii of the drops are comparable to the size of the tube, and the drops adopt an eccentric lateral position owing to a density difference between the drop and the suspending fluid. Measured values for the extra pressure difference caused by the presence of the drop, the relative velocity of the drop, and the shape of the drop are correlated with the minimum gap width between the eccentrically located drop and the tube wall using simple lubrication approximations. The viscosity ratio, density difference, volumetric flow rate and drop size are varied in the experiment. Comparisons with previous results for concentric, neutrally buoyant drops show that the effects of eccentric position can be substantial for surprisingly small values of the density difference. Both Newtonian and viscoelastic suspending fluids are considered, and the results suggest that both viscometric and time-dependent non-Newtonian effects are present. For the Newtonian case, the data are compared with the predictions of available theories which account explicitly for the eccentric drop position.

## 1. Introduction

The creeping motion of drops suspended in a tube flow is important as a prototype problem in many industrial and biological processes. Immiscible additives, in the form of small particles or drops, are often used in polymer-melt processing to alter the bulk properties of the final product; it is crucial that the kinematics and dynamics of the resulting two-phase flow be understood if the desired structure is to be achieved. The well-known analogy between the motion of large droplets through tubes and the creeping motion of erythrocytes through capillaries has also served as a motivation for many earlier studies of this problem. Although there are recent studies, e.g. Tozeren & Skalak (1978), that present experimental and theoretical models for capillary blood flow which are far more realistic than the simple system considered here, the sensitivity of the results to density differences between the two phases has not been examined; and for this reason, the present study may still be of qualitative interest in the blood-flow problem. Our own motivation for the general study, of which this present work is a part, is the development of a realistic laboratory model for investigation of the microdynamics of two-phase flows in porous media (i.e. the

† Present address: School of Chemical Engineering, Cornell University, Ithaca, New York 14853.

dynamics at the scale of the pores). This problem is of interest in tertiary oil recovery methods including polymeric and surfactant flooding. Here, oil droplets are displaced and carried by a so-called 'pusher' fluid through the porous matrix toward a collection well. Much of the effort in making this process feasible has concerned an understanding of the dynamics at the scale of the whole reservoir. The present investigations are aimed at an understanding of the detailed dynamics at the scale of the individual flow channel. Specifically, we aim ultimately to achieve a more fundamental grasp of the relationships between 'dependent' parameters such as the flow resistance, drop mobility or stable drop size (i.e. drop break-up), and 'independent' parameters of the system such as fluid properties, channel geometry and interfacial tension.

One system which has been proposed as a model for studying flow in porous media is a tube with axially varying cross-sectional area (cf. Neira & Payatakes 1979; Fedkiw & Newman 1977; Payatakes & Neira 1977; Deiber & Schowalter, 1979). Although the periodically constricted tube is a gross oversimplification of the flow-channel geometry in a porous medium, it does allow some of the effects associated with a rapidly varying cross-sectional area to be investigated. In an earlier paper, Ho & Leal (1975) considered the case of neutrally buoyant drops in a straight-walled tube for both Newtonian and viscoelastic suspending fluids. The straight-walled tube problem is of some intrinsic interest in its own right, and is a necessary preliminary to the investigation of the wavy-walled tube flow. Here, we consider the effect of differences in density between the drops and the suspending fluid, again for creeping motion through a straight, circular, horizontal tube. In an accompanying paper (Olbricht & Leal 1981), the effects of flow-channel geometry will be investigated.

In the present experiments we measure: the incremental pressure difference $\Delta P^+$ required to maintain a specified flow rate relative to that required for the suspending fluid alone; the velocity $U$ of the drops relative to the average velocity of the two-phase flow $V$; the shapes of the drops; and the minimum gap width $h$ between the lower surface of the drops and the tube wall. In the context of two-phase flow through porous media, $\Delta P^+$ is related to the accessibility of individual channels to flow compared to channels which contain no drops (i.e. the microscale 'sweep efficiency'), $U$ is a measure of the drop mobility, and the shape is important as a precursor to dispersion (break-up) processes. The major focus of the present experiments is the effect of the lateral position of the drop in the horizontal tube as a consequence of density differences between the two fluids.

The present study is focused on a determination of the sensitivity of $\Delta P^+$, $U$ and drop shape to small density differences between the two phases, and a delineation of the domain where non-neutral buoyancy is a significant factor. The relevant *independent* dimensionless parameters for the experiment include: $\lambda$, the undeformed drop radius relative to the radius of the tube $R_0$; $\sigma$, the ratio of the drop fluid viscosity $\mu_i$ to that of the suspending fluid $\mu_0$; a deformation parameter which is the inverse of the so-called capillary number $\Gamma = \mu_0 V/\gamma$, where $\gamma$ is the interfacial tension between the drop and suspending fluid; and $\Delta\rho/\rho_0$, where $\Delta\rho$ is the difference between the specific gravity of the drop fluid $\rho_i$ and that of the suspending fluid $\rho_0$. In the case of a viscoelastic suspending fluid, the results will also depend on the dimensionless parameters which characterize the rheological properties of the fluid. Foremost among these is the Deborah number $De = \theta/\tau$, where $\theta$ is the intrinsic

relaxation time for the fluid ($\theta = 0$ in a Newtonian fluid) and $\tau$ is a time scale for the variation of the deformation rate. In the experimental data which are presented in § 3, the additional pressure drop $\Delta P^+$ is scaled by the characteristic viscous pressure $\mu_0 V/R_0$.

Existing theories for the motion of particles through tubes are largely concerned with Newtonian suspending fluids. The effect of an eccentric position of the drop has been considered in only two previous studies. Hetsroni, Haber & Wacholder (1970) used the method of reflections to solve for the velocity fields associated with the motion of a small, spherical (undeformed) drop which is not too near a wall in a Poiseuille flow. The lateral position of the drop is specified, in dimensionless terms, by $\beta = b/R_0$, where $b$ is the distance between the centre line of the tube and the centre of the undeformed drop. The relative velocity of the drop for this case is predicted to be

$$\frac{U}{V} = 2(1-\beta^2) - \frac{4\sigma}{3\sigma+2}\lambda^2 + O(\lambda^3). \tag{1}$$

Brenner (1973) used the reciprocal theorem for creeping flow to obtain the additional pressure drop for this flow:

$$\frac{\Delta P^+ R_0}{\mu_0 V} = \frac{16[(9\sigma+2)^2-40]}{27(\sigma+1)(3\sigma+2)}\lambda^5 + \frac{32(5\sigma+2)}{3(\sigma+1)}\beta^2\lambda^3 + O(\lambda^6). \tag{2}$$

Later, Bungay & Brenner (1973*a*) also obtained results for a small rigid sphere near the tube wall. It will be noted that (1) and (2) contain the lateral position of the drop explicitly through $\beta$. Unfortunately, though $\beta$ depends mainly on the density difference, $\Delta\rho/\rho_0$ in the present experiments, its value has not been predicted in any of the existing theoretical developments. Thus, quantitative comparisons between the data for $U$ and $\Delta P^+$ and the predictions from (1) and (2), respectively, can be made only by estimating the value of $\beta$ directly from photographs of the drops in the flow.

Some theoretical work has also been done for particles which are of a size similar to that of the tube, but only for neutrally buoyant, concentrically located particles. Hyman & Skalak (1972*a*, *b*) calculated $\Delta P^+$ and $U$ for deformable and non-deformable liquid drops, while Bungay & Brenner (1973*b*) considered the case of close-fitting rigid spheres. Lighthill (1968) and Fitz-Gerald (1969) also studied the motion of a large elastic particle, but evaluation of $\Delta P^+$ is difficult from their results, and the calculation was subsequently improved, for the axisymmetric case, by Tozeren & Skalak (1978). As noted above, no theoretical work has so far been done which considers *large* eccentrically positioned particles.

Finally, we mention briefly earlier experimental investigations which are related to the present work. These include Hochmuth, Marple & Sutera (1970), Sutera *et al.* (1970), Seshardi *et al.* (1970), and Hochmuth & Sutera (1970), and involve the motions of erythrocytes, model cells, and spherical caps in Newtonian fluids through capillary tubes. Prothero & Burton (1961, 1962) studied qualitatively the motion of gas bubbles in a Newtonian liquid, once again as a model for blood flow. Goldsmith & Mason (1963) reported $U$ and $h$ for very large drops ($\lambda \gg 1$) in creeping flow. However, none of these experimental studies includes the effects of non-neutral buoyancy.

The case of a viscoelastic suspending fluid has received scant attention in the literature, apart from the paper by Ho & Leal (1975) cited earlier. Indeed, the only

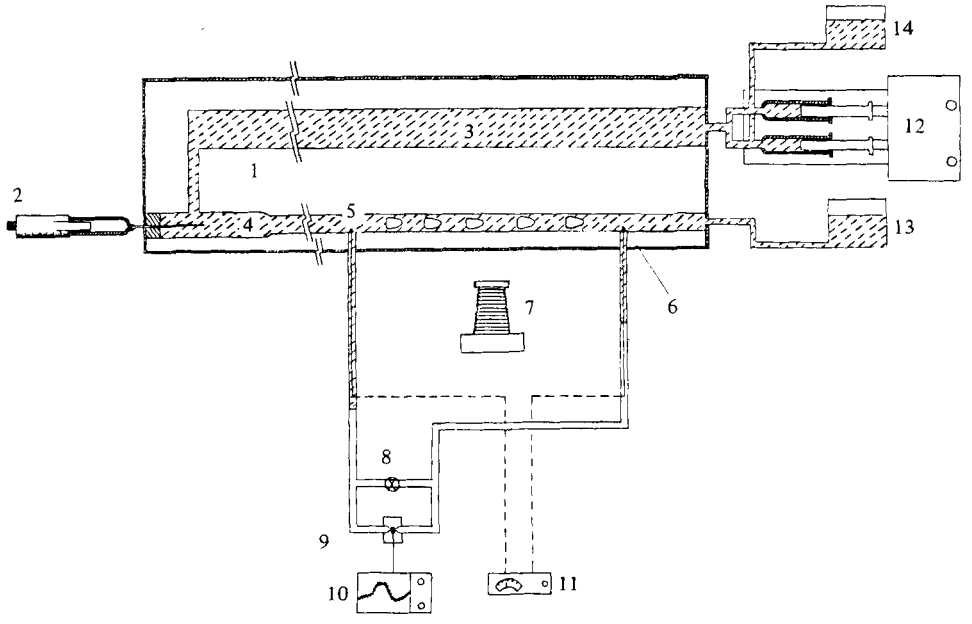


FIGURE 1. Schematic diagram of the apparatus (not to scale). (1) Constant-temperature bath. (2) Micrometer syringe. (3) Suspending-fluid storage section. (4) Test section. (5) Pressure port. (6) Pressure port. (7) Camera. (8) Manometer by-pass valve. (9) Pressure transducer. (10) Transducer indicator. (11) Thermocouple. (12) Pump: syringe or gear type. (13) Waste storage. (14) Suspending-fluid reservoir.

other work which is at all relevant to the present paper is that of Sigli & Coutanceau (1977), who measured the drag on rigid spheres falling through a cylindrical tube, when the particle and tube are of comparable diameter. The data show significant qualitative effects of fluid viscoelasticity when the interaction between the particle and the tube wall is important, even though the nominal Deborah number is small.

## 2. Experimental apparatus and materials

The apparatus used in this experiment is similar to the one used in Ho & Leal (1975) and is illustrated in figure 1. The flow was driven by one of two available pumps capable of maintaining a constant flow rate with less than 0·1 % variation over the course of a single experimental run. For the Newtonian suspending fluid, a Harvard Apparatus infusion/withdrawal syringe pump was used, while a Zenith Products Series BPB gear pump was employed with the more 'viscous' viscoelastic suspending fluid.

The suspending fluid was held in an overhead reservoir before entering the pump. Fluid was then pumped into a large storage section which was immersed in a constant-temperature bath maintained at $25 \pm 0{\cdot}1$ °C. The transit time through this storage section was always sufficiently long to ensure that the temperature of the suspending fluid had equilibrated with the bath before entering the test section. The test section consisted of a horizontal precision-bore glass tube with a diameter of 1 cm and a length of 120 cm. Pressure ports were positioned 50 cm apart, the first port being 50 cm downstream from the entrance to the test section. After passing through the

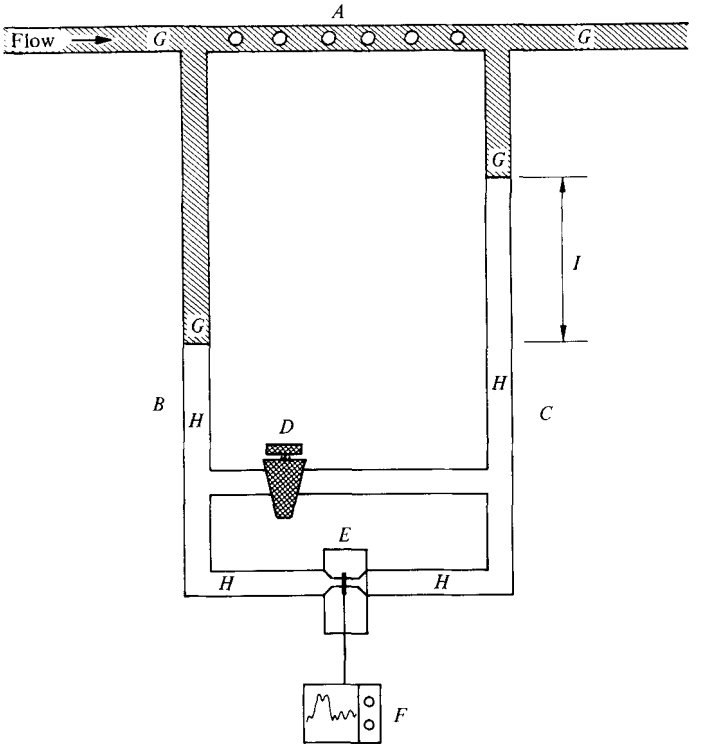


FIGURE 2. Schematic diagram of manometer–transducer system (not to scale). (*A*) Test section. (*B*) Upstream manometer leg. (*C*) Downstream manometer leg. (*D*) By-pass valve. (*E*) Pressure transducer. (*F*) Transducer indicator and recorder. (*G*) Suspending fluid. (*H*) Carbon tetrachloride. (*I*) Pressure difference due to suspending fluid alone.

test section, the fluid left the controlled-temperature region and was held in a storage container.

The drops were manually injected upstream of the test section using a Hamilton precision micrometer syringe capable of producing drops of known volume to within 0·001 ml. The micrometer syringe was connected to a flexible tube fitted at its end with a 15-gauge hypodermic needle. The needle was inserted directly into the flow through a fitting containing a rubber septum. The drops were injected with the pump operating at a low speed so that they would detach from the needle shortly after injection. Once all the drops for a particular run had been injected, the pump was adjusted to the full desired flow rate. It was found that the drops attained an equilibrium position in the tube well before entering the region between the pressure ports. The equilibrium position was found to depend on all the material and flow parameters, but most strongly on the density difference between the drop and suspending fluid. Furthermore, the equilibrium position was completely independent of the initial lateral position of injection.

The pressure ports were connected to a differential manometer/transducer system capable of detecting changes in the pressure difference down to approximately $10^{-3}$ in. of water. This level of sensitivity is important because the extra pressure difference due to the presence of a drop in the flow can sometimes be exceedingly small. The

manometer/transducer system is shown schematically in figure 2. Since the total fall in pressure between the pressure ports was much larger than the full-scale sensitivity of the transducer (a Validyne Engineering Co. Model DP45 with a full-scale range of only 0·5 in. of water), the manometer was used to balance the (major) portion of the fall in pressure due to the flow of the suspending fluid alone. The transducer then detected only the relatively small changes in the pressure difference due to the presence of the drop (or drops) in the test section. The details of this procedure were outlined in Ho & Leal (1975).

The velocity of a drop was also independent of spacing when the drops were separated by at least one tube diameter and was measured by determining visually the time for transit between known points in the tube. The volumetric flow rate $Q$ was determined by collecting a measured volume of fluid from the outlet of the test section over a measured time interval. Photographs were taken while the drops were in the test section between the pressure taps using a 35 mm Pentax camera fitted with a close-up lens. The refractive index of the fluid in the constant-temperature circulating bath was matched with the refractive index of the suspending fluid in the manner outlined in Ho & Leal, and this minimized distortion in the photographs due to the curved surface of the tube.

The Newtonian suspending fluid was 95·75% (w/w) glycerine in water. The density of the solution, measured with a hydrometer, was found to be $1{\cdot}251 \pm 0{\cdot}001$ g/cm$^3$ during the course of the experiment. The viscosity was also monitored during the runs, but was always found to be $4{\cdot}17 \pm 0{\cdot}02$ P. The slight variation is due primarily to 0·1 °C variations in temperature in the circulating water bath.

The viscoelastic suspending fluid was a 0·5% w/w aqueous solution of Dow Separan AP30, a polydisperse polyacrylamide with rheological properties that have been extensively studied (Leal, Skoog & Acrivos 1971; Huppler *et al.* 1967*a*, *b*). One difficulty in comparing experimental results for the Newtonian and viscoelastic suspending fluids is to determine an appropriate viscosity for the Separan solutions since these show a strong shear-thinning effect. However, we follow the precedent of Ho & Leal (1975) and simply evaluate the viscosity at the wall-shear rate for the undisturbed flow using a power-law model ($n = 0{\cdot}45$) to estimate the shear-thinning behaviour of the fluid. The resulting values of the suspending fluid viscosity at the flow rates for the present experiment can be determined from table 1. Unfortunately, the viscoelastic fluid viscosity was found to vary significantly from batch to batch of the Separan solution. Although care was taken to prepare each batch of suspending fluid in an identical manner, variations in the fluid viscosity up to 10% appeared to be unavoidable.

In addition to a shear-thinning viscosity and normal-stress differences in simple shear flow, dilute polymer solutions exhibit a finite response time in unsteady (Lagrangian or Eulerian) flow. This characteristic time is associated with the fluid's adjustment at the macromolecular level to a change in the bulk deformation gradient. When the fluid time scale is comparable to the characteristic time scale of a flow, the response of the system may be governed, at least in part, by the relative magnitude of these time scales, i.e. $De = \theta/\tau$.

As far as the present experiment is concerned, if the suspended drop were sufficiently small, it would move with the local fluid velocity, and hence the flow would be steady everywhere. Furthermore, the flow field at any point would be

| System | Suspending fluid | Drop-fluid viscosity (P) | $\Delta\rho/\rho_0$ | Viscosity ratio, $\sigma$ | | | Deformation parameter $\Gamma \equiv \mu_0 V/\gamma$ | | |
|---|---|---|---|---|---|---|---|---|---|
| | | | | $V$ = 0·32 (cm/s) | $V$ = 0·56 (cm/s) | $V$ = 0·80 (cm/s) | $V$ = 0·32 (cm/s) | $V$ = 0·56 (cm/s) | $V$ = 0·80 (cm/s) |
| 2 | Glycerine/water | 11·0 | 0·020 | 2·63 | 2·63 | 2·63 | 0·061 | 0·11 | 0·15 |
| 3 | | 3·21 | 0·018 | 0·77 | 0·77 | 0·77 | 0·061 | 0·11 | 0·15 |
| 4 | | 1·25 | 0·011 | 0·30 | 0·30 | 0·30 | 0·061 | 0·11 | 0·15 |
| 5 | | 1·47 | 0·038 | 0·35 | 0·35 | 0·35 | 0·061 | 0·11 | 0·15 |
| 6 | | 11·1 | 0·037 | 2·68 | 2·68 | 2·68 | 0·061 | 0·11 | 0·15 |
| 2V | 0·5% Separan | 20·0 | 0·039 | 3·1 | 4·3 | 5·1 | 0·08 | 0·10 | 0·12 |
| 2V | | 5·34 | 0·038 | 0·74 | 0·87 | 1·2 | 0·08 | 0·13 | 0·14 |
| 4V | | 2·06 | 0·037 | 0·32 | 0·44 | 0·52 | 0·08 | 0·10 | 0·12 |
| 5V | | 0·59 | 0·038 | 0·090 | 0·13 | 0·15 | 0·08 | 0·10 | 0·12 |
| 6V | | 19·5 | 0·019 | 2·9 | 3·8 | 4·6 | 0·08 | 0·10 | 0·12 |
| 7V | | 0·55 | 0·019 | 0·080 | 0·11 | 0·13 | 0·08 | 0·11 | 0·13 |
| 8V | | 1·82 | 0·018 | 0·23 | 0·31 | 0·39 | 0·09 | 0·12 | 0·13 |
| 9V | | 5·24 | 0·018 | 0·70 | 0·94 | 1·2 | 0·09 | 0·12 | 0·13 |

TABLE 1. Properties of the materials

| Drop volume (cm³) | $\lambda$ |
|---|---|
| 0·070 | 0·512 |
| 0·100 | 0·576 |
| 0·150 | 0·660 |
| 0·200 | 0·726 |
| 0·250 | 0·782 |
| 0·300 | 0·831 |

| Volumetric flow rate (cm³/min) | $V$ (cm/s) |
|---|---|
| 15·0 | 0·32 |
| 26·4 | 0·56 |
| 37·7 | 0·80 |

TABLE 2. Flow parameters

nearly simple shear flow, and consequently the non-Newtonian properties could be described completely by variations in the viscosity and the normal stresses in a viscometric flow. However, the drop is not asymptotically small in the present experiments and thus travels at a velocity which differs from the local suspending-fluid velocity. As a result, fluid elements experience a local acceleration as they move around the drop. This unsteadiness is a possible source of time-dependent non-Newtonian effects. The importance of such effects can be measured by *De*. The appropriate timescale for the flow is approximately $2D\lambda R_0/(U-V)$, where the difference in velocity between the drop and the surrounding suspending fluids is estimated to be $U-V$, and $2D\lambda R_0$ is the 'length' of the deformed drop (see § 3). The characteristic time for the fluid can be estimated from steady-shear-flow data, employing a constitutive model to relate $\theta$ to normal-stress measurements. We have used the contravariant form of the convected Maxwell model for this purpose, and $\theta$ has been evaluated at the wall-shear rate. Our estimates show that the maximum value of *De* under the conditions of the present experiment is approximately 0·20. Most previous experimental evidence suggests that time-dependent non-Newtonian effects are only significant when $De \geqslant 1$–2. Thus, we expect to be able to interpret the experimental results reported here largely in terms of steady flow behaviour for the fluid.

The drops consisted of solutions of Dow Corning silicone oil mixed with carbon tetrachloride. The values of $\sigma = \mu_i/\mu_0$ and $\Gamma = \mu_0 V/\gamma$ for the systems used are listed in table 1. The density differences employed in this study were small, never exceeding 0·04 g/cm³. Nevertheless, the changes induced over this range of $\Delta\rho$ are both qualitatively and quantitatively significant. Indeed, this range is apparently sufficient to expose the asymptotic behaviour for 'large' values of $\Delta\rho$ in such quantities as $\Delta P^+ R_0/\mu_0 V$ or $U/V$. These are important findings, since density differences of this magnitude are likely to be common in many systems of interest, in spite of the fact that *no* account has been taken of them in the majority of existing theoretical studies. The analysis of Hyman & Skalak (1972*b*), mentioned in § 1, provides a good example. Calculations were made for $\Delta P^+$ and $U$ for liquid drops taken as a model of erythrocytes in capillaries. It was assumed that the drops were neutrally buoyant and concentrically located, even though the authors point out that the density of

| | System | | | | | | | | | | | |
|---|---|---|---|---|---|---|---|---|---|---|---|---|
| $\lambda$ | 2 | 3 | 4 | 5 | 6 | 2V | 3V | 4V | 5V | 6V | 7V | 8V | 9V |
| | | | | | | ($V$ = 0·32 cm/s) | | | | | | | |
| 0·512 | 1·99 | 1·48 | 0·06 | 1·01 | 1·99 | 0·70 | 0·79 | 0·47 | 0·90 | 0·34 | 0·28 | 0·20 | 0·17 |
| | 1·41 | 1·38 | 1·71 | 1·37 | 1·20 | 1·44 | 1·44 | 1·45 | 1·40 | 1·50 | 1·52 | 1·50 | 1·50 |
| 0·577 | 2·22 | 1·48 | 0·94 | 1·82 | 3·22 | 0·93 | 0·86 | 0·82 | 1·12 | 0·41 | 0·46 | 0·42 | 0·41 |
| | 1·49 | 1·49 | 1·66 | 1·41 | 1·29 | 1·39 | 1·43 | 1·41 | 1·38 | 1·46 | 1·48 | 1·46 | 1·47 |
| 0·660 | 2·89 | 1·68 | 1·12 | 1·62 | 3·54 | 1·23 | 1·23 | 1·23 | 1·35 | 0·93 | 0·91 | 0·78 | 0·78 |
| | 1·49 | 1·46 | 1·58 | 1·44 | 1·34 | 1·34 | 1·40 | 1·38 | 1·36 | 1·40 | 1·42 | 1·41 | 1·41 |
| 0·726 | 4·10 | 2·88 | 1·13 | 1·60 | 4·68 | 1·75 | 1·56 | 1·82 | 1·89 | 1·42 | 1·79 | 1·37 | 1·35 |
| | 1·43 | 1·40 | 1·52 | 1·43 | 1·36 | 1·32 | 1·36 | 1·34 | 1·34 | 1·36 | 1·37 | 1·36 | 1·35 |
| 0·782 | 4·68 | 3·12 | 1·25 | 2·26 | 5·20 | 2·10 | 1·93 | 2·45 | 2·50 | 2·51 | 2·39 | 1·98 | 2·12 |
| | 1·41 | 1·37 | 1·47 | 1·41 | 1·34 | 1·30 | 1·34 | 1·30 | 1·30 | 1·31 | 1·32 | 1·32 | 1·32 |
| 0·831 | 6·06 | 4·19 | 1·96 | 2·14 | 6·24 | 2·80 | 2·62 | 3·20 | 2·96 | 2·80 | 2·95 | 2·63 | 2·77 |
| | 1·37 | 1·32 | 1·42 | 1·38 | 1·33 | 1·28 | 1·31 | 1·27 | 1·28 | 1·27 | 1 29 | 1·28 | 1·27 |
| | | | | | | ($V$ = 0·56 cm/s) | | | | | | | |
| 0·512 | 1·49 | 0·97 | 0·00 | 0·71 | 1·56 | 0·44 | 0·40 | 0·30 | 0·43 | 0·19 | 0·22 | 0·19 | 0·15 |
| | 1·54 | 1·61 | 1·77 | 1·49 | 1·36 | 1·46 | 1·50 | 1·47 | 1·47 | 1·50 | 1·50 | 1·50 | 1·51 |
| 0·577 | 2·18 | 1·03 | 0·23 | 0·65 | 2·20 | 0·56 | 0·56 | 0·53 | 0·64 | 0·32 | 0·34 | 0·37 | 0·27 |
| | 1·57 | 1·62 | 1·73 | 1·53 | 1·40 | 1·43 | 1·46 | 1·45 | 1·44 | 1·47 | 1·47 | 1·47 | 1·47 |
| 0·660 | 2·38 | 1·46 | 0·25 | 0·68 | 2·49 | 1·00 | 0·89 | 0·87 | 1·02 | 0·71 | 0·71 | 0·68 | 0·65 |
| | 1·56 | 1·58 | 1·68 | 1·54 | 1·42 | 1·41 | 1·42 | 1·41 | 1·40 | 1·41 | 1·42 | 1·42 | 1·42 |
| 0·726 | 3·37 | 2·10 | 0·39 | 0·89 | 2·97 | 1·36 | 1·28 | 1·53 | 1·46 | 1·16 | 1·12 | 1·05 | 1·10 |
| | 1·55 | 1·51 | 1·60 | 1·50 | 1·40 | 1·37 | 1·38 | 1·38 | 1·36 | 1·37 | 1·38 | 1·38 | 1·37 |
| 0·782 | 4·19 | 2·72 | 0·32 | 0·89 | 3·79 | 1·95 | 1·78 | 1·97 | 2·00 | 1·81 | 1·79 | 1·62 | 1·67 |
| | 1·47 | 1·47 | 1·54 | 1·49 | 1·39 | 1·34 | 1·34 | 1·34 | 1·32 | 1·33 | 1·34 | 1·33 | 1·33 |
| 0·831 | 4·84 | 3·72 | 0·13 | 0·97 | 4·09 | 2·62 | 2·44 | 2·51 | 2·93 | 2·57 | 2·35 | 2·00 | 2·31 |
| | 1·44 | 1·44 | 1·50 | 1·46 | 1·36 | 1·32 | 1·32 | 1·30 | 1·30 | 1·30 | 1·30 | 1·31 | 1·30 |
| | | | | | | ($V$ = 0·80 cm/s) | | | | | | | |
| 0·512 | 1·15 | 0·67 | 0·07 | 0·45 | 0·89 | 0·34 | 0·31 | 0·31 | 0·33 | 0·17 | 0·18 | 0·18 | 0·19 |
| | 1·60 | 1·63 | 1·79 | 1·57 | 1·43 | 1·49 | 1·50 | 1·51 | 1·49 | 1·50 | 1·50 | 1·50 | 1·51 |
| 0·577 | 1·55 | 0·86 | 0·17 | 0·54 | 2·08 | 0·62 | 0·42 | 0·41 | 0·40 | 0·25 | 0·35 | 0·30 | 0·27 |
| | 1·59 | 1·66 | 1·75 | 1·57 | 1·47 | 1·46 | 1·47 | 1·47 | 1·46 | 1·47 | 1·47 | 1·47 | 1·47 |
| 0·660 | 2·09 | 0·93 | 0·11 | 0·52 | 2·43 | 1·05 | 0·74 | 0·66 | 0·74 | 0·59 | 0·66 | 0·58 | 0·65 |
| | 1·58 | 1·58 | 1·68 | 1·56 | 1·47 | 1·41 | 1·43 | 1·42 | 1·43 | 1·42 | 1·43 | 1·43 | 1·44 |
| 0·726 | 3·22 | 1·68 | −0·10 | 0·65 | 2·50 | 1·40 | 1·10 | 0·69 | 1·16 | 0·93 | 1·01 | 0·95 | 1·08 |
| | 1·53 | 1·54 | 1·65 | 1·55 | 1·47 | 1·37 | 1·41 | 1·38 | 1·38 | 1·37 | 1·40 | 1·38 | 1·39 |
| 0·782 | 3·92 | 1·45 | −0·22 | 0·69 | 3·72 | 2·26 | 1·56 | 1·15 | 1·70 | 1·49 | 1·55 | 1·32 | 1·54 |
| | 1·47 | 1·50 | 1·59 | 1·51 | 1·44 | 1·34 | 1·36 | 1·34 | 1·34 | 1·34 | 1·35 | 1·36 | 1·35 |
| 0·831 | 4·42 | 1·87 | −0·50 | 0·50 | 3·83 | 2·56 | 1·90 | 1·95 | 2·13 | 2·31 | 2·06 | 1·51 | 2·06 |
| | 1·44 | 1·48 | 1·56 | 1·49 | 1·42 | 1·29 | 1·35 | 1·32 | 1·31 | 1·31 | 1·32 | 1·35 | 1·32 |

TABLE 3. Data for $\Delta P^+$ and $U/V$. For each system, drop size and flow rate there are a pair of numbers. The upper is the measured value for $\Delta P^+ R_0/\mu_0 V$ and the lower is the measured value for $U/V$.

erythrocytes differs from that of the suspending plasma by 0·07 g/cm$^3$. The neglect of even relatively small density differences may turn out to be a significant shortcoming of this and similar calculations.

The dimensionless parameter $\Gamma$ characterizes the relative magnitude of viscous stresses as compared to interfacial tension forces at the drop surface, and is the inverse of what is often called the capillary number. This parameter was varied in

the present experiments through variations in the flow rate $V$. The interfacial tension $\gamma$ was measured using a duNuoy ring tensiometer. The measured values are 22 dyn/cm and 26 dyn/cm for silicone oil drops with the Newtonian and viscoelastic suspending fluids, respectively.

The flow parameters, namely the size of the drops and the flow rates used in this experiment, are listed in Table 2.

## 3. Experimental results

Measurements of $\Delta P^+$, $U$, shape, and distance from the wall $h$ have been made for the thirteen systems listed in table 1. The material properties of each system, namely the drop viscosity and density, were chosen so that comparisons between them would reveal the effects of the individual variables on the dependent quantities, such as $\Delta P^+$ or $U$. Furthermore, comparisons between selected Newtonian and viscoelastic suspending fluid systems reveal the qualitative effects of viscoelasticity on the measured quantities. Finally, comparison with the corresponding results of Ho & Leal (1975) for neutrally buoyant drops provides a further indication of the effects of density differences between the two fluids. Measurements were made for each system for three flow rates ($0{\cdot}3 \leqslant V \leqslant 0{\cdot}8$ cm/s) and for six drop sizes ($0{\cdot}5 \leqslant \lambda \leqslant 0{\cdot}8$). Thus, two material properties, $\sigma$ and $\Delta\rho$, and two 'flow parameters', $V$ and $\lambda$, have been independently varied. The main results are presented in four parts, organized according to the specific property which is being varied, rather than the quantity being measured. This scheme of presentation facilitates discussion of the results, since the variation of a single experimental parameter often affects more than one measured quantity. Mechanistic explanations for the results are proposed whenever possible, and the ranges of their validity over the parameter space are estimated. In addition, the data are compared in § 5 to the small-$\lambda$ theories of Brenner (1973) for $\Delta P^+$ and Hetsroni *et al.* (1970) for $U$, which account explicitly for the eccentricity of the drop's position in the tube.

The data for $\Delta P^+ R_0/\mu_0 V$ and $U/V$ for each size drop and each flow rate are tabulated in table 3. In an attempt to characterize the degree of drop deformation, a parameter $D$ was defined as the maximum linear dimension of the drop (as measured from photographs) rendered dimensionless by the undeformed drop diameter $2\lambda R_0$. Clearly, the parameter $D$ is insufficient to describe the detailed shapes assumed by the drops during flow, since the drops exhibit neither fore/aft symmetry, nor axisymmetry when $\Delta\rho \neq 0$. Nevertheless, measurements of $D$ will be useful for the purpose of comparison between various systems. Representative data for $D$ and the minimum gap width $h$ between the lower surface of the drop and the tube wall will be presented later in this section. A complete accounting of numerical values for $D$ and $h$ is given by Olbricht (1980).

Let us now turn to a detailed examination of the data. In this section, we focus simply on the dependence of such variables as $\Delta P^+$, $U/V$ and $D$ on the independent parameters, $\Gamma$, $\sigma$, $\lambda$ and $\Delta\rho/\rho_0$. The results are then discussed in § 4 with the objective of obtaining a qualitative understanding of the underlying physical mechanisms.

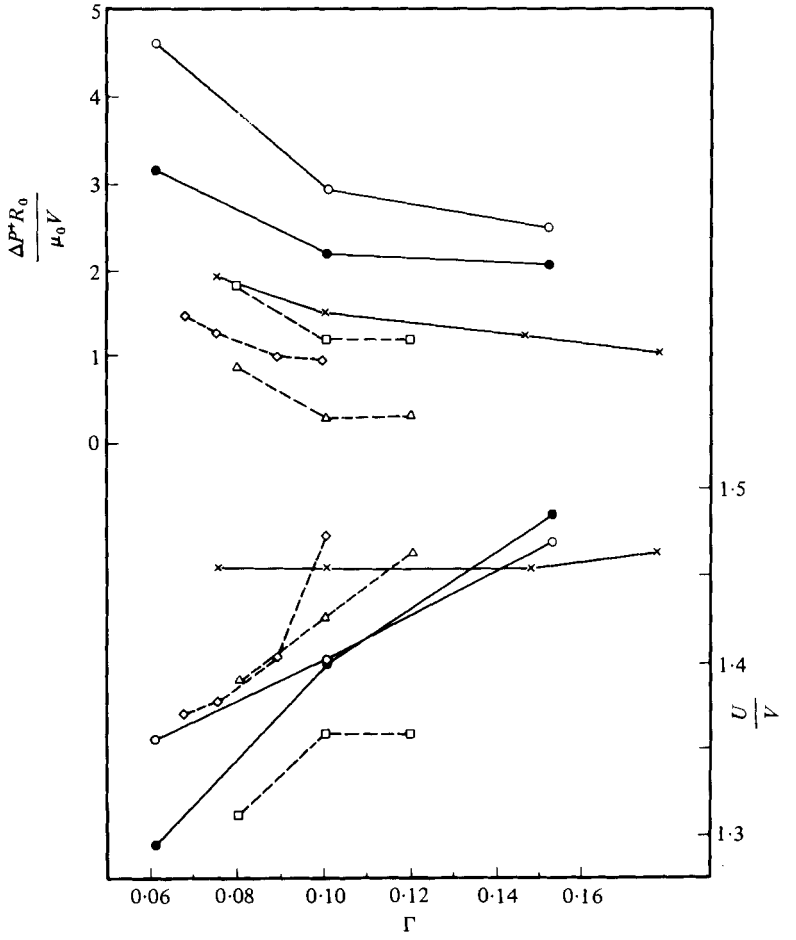


FIGURE 3. Dimensionless extra pressure difference and relative velocity as functions of $\Gamma$ ($= u_0 V/\gamma$). ○, System 6 (Newtonian): $\sigma = 2{\cdot}68$, $\Delta\rho/\rho_0 = 0{\cdot}037$, $\lambda = 0{\cdot}726$. ●, System 6 (Newtonian): $\sigma = 2{\cdot}68$, $\Delta\rho/\rho_0 = 0{\cdot}037$, $\lambda = 0{\cdot}576$. □, System 2V (viscoelastic): $\sigma = 3{\cdot}1$–$5{\cdot}1$, $\Delta\rho/\rho_0 = 0{\cdot}039$, $\lambda = 0{\cdot}726$. △, System 2V (viscoelastic): $\sigma = 3{\cdot}1$–$5{\cdot}1$, $\Delta\rho/\rho_0 = 0{\cdot}039$, $\lambda = 0{\cdot}576$. ×, (Newtonian): $\sigma = 2{\cdot}04$, $\Delta\rho/\rho_0 = 0$, $\lambda = 0{\cdot}726$ (from Ho & Leal 1975). ◇, (viscoelastic): $\sigma = 3{\cdot}1$–$5{\cdot}1$, $\Delta\rho/\rho_0 = 0$, $\lambda = 0{\cdot}726$ (from Ho & Leal 1975).

### 3.1. *Average velocity*

Let us first consider effects of the bulk flow rate or, equivalently, the average velocity $V$ for fixed values of $\lambda$, $\sigma$, and $\Delta\rho/\rho_0$. A dimensional analysis of the problem for $Re$ ($= \rho_0 R_0 V/\mu_0$) $\ll 1$ shows that the primary effects of the bulk velocity in the case of a Newtonian suspending fluid should be manifested through variations in the parameter $\Gamma = \mu_0 V/\gamma$. In the case of a viscoelastic suspending fluid, the rheological properties also depend upon the magnitude (and form) of the velocity gradient tensor and this provides the potential for additional dependence on $V$. The effects of $V$ on $\Delta P^+ R_0/\mu_0 V$ and on $U/V$ for both Newtonian and viscoelastic fluid systems are illustrated in figure 3, where $\Delta P^+ R_0/\mu_0 V$ and $U/V$ are plotted as functions of $\Gamma$ for several systems which have approximately the same values of $\sigma$ and $\lambda$. The differences between the two non-neutrally buoyant Newtonian systems are a

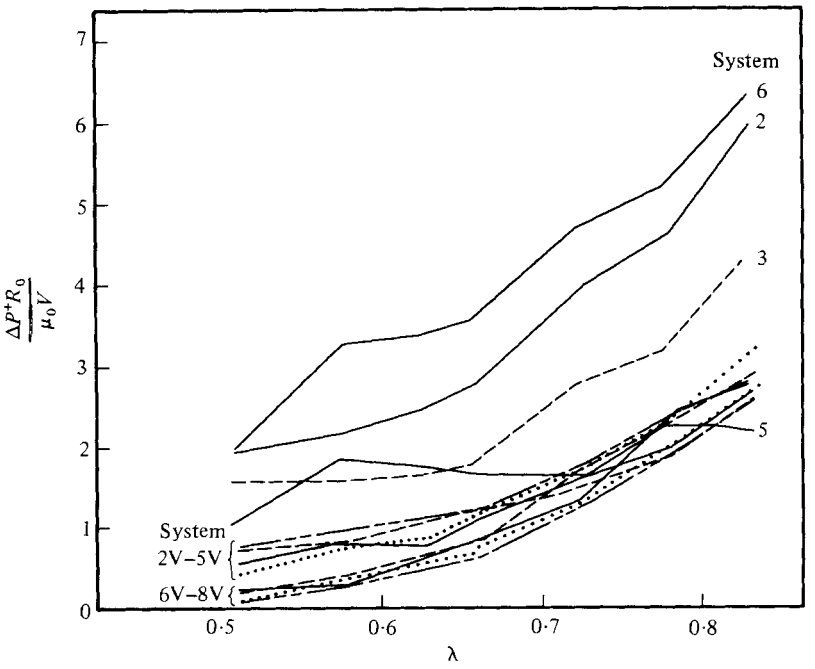


FIGURE 4. Dimensionless extra pressure difference as a function of $\lambda$. Shown are Newtonian systems **2**, **3**, **5**, **6** and all viscoelastic systems for $V = 0{\cdot}32$ cm/s.

consequence of the difference in drop size ($\lambda = 0{\cdot}58$ and $\lambda = 0{\cdot}73$, respectively), and this is also true of the two non-neutrally buoyant viscoelastic fluid cases. A systematic discussion of the dependence of $\Delta P^+ R_0/\mu_0 V$ and $U/V$ on $\lambda$ will be presented later. The effect of increasing $\Gamma$, in all cases considered here, is to cause the dimensionless additional pressure difference $\Delta P^+ R_0/\mu_0 V$ to decrease, and the relative mobility of the drop $U/V$ to increase. In general, it appears that $\Delta P^+ R_0/\mu_0 V$ approaches a constant asymptotic value for the highest flow rates, though this is *not* true of the mobility over the range of $\Gamma$ considered here.

In addition, we may note that increases in $\Gamma$ also led to increases in the drop deformation $D$ and in the gap width $h$, for both Newtonian and viscoelastic suspending fluids.

All of these effects of increased average velocity are slightly more dramatic for larger drops. Furthermore, the identical qualitative trends are observed for both neutrally buoyant and non-neutrally buoyant drops, indicating that drop eccentricity is not an important factor with regard to flow-rate variations.

### 3.2. *Drop size*

The effects of drop size were studied for each system by taking measurements for six different sizes, $0{\cdot}51 \leqslant \lambda \leqslant 0{\cdot}83$. The larger sizes are directly comparable to those chosen in Ho & Leal (1975) for neutrally buoyant drops. Although it is impossible to illustrate all of the data, figure 4 provides an indication of the dependence of $\Delta P^+$ on $\lambda$ for systems with $\Delta\rho/\rho_0 \simeq 0{\cdot}04$. Let us now consider these results in detail, beginning with the Newtonian suspending fluid systems.

*Newtonian suspending fluid.* The dependence of the additional pressure difference

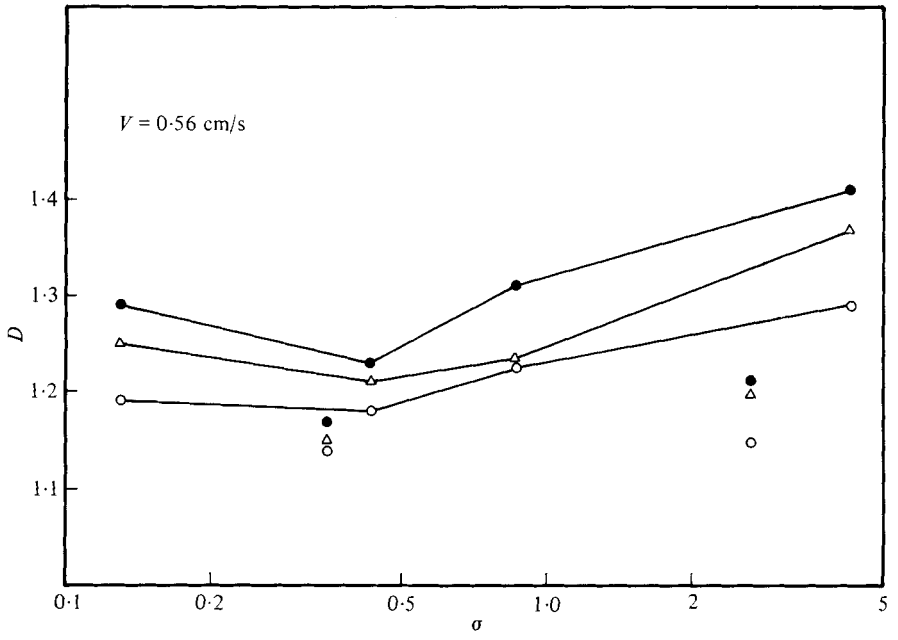


FIGURE 5. $D$ (= largest linear dimension/undeformed diameter) as a function of viscosity ratio for $V = 0{\cdot}56$ cm s$^{-1}$, and three dimensionless drops sizes: ●, $\lambda = 0{\cdot}83$; △, 0·72; ○, 0·63. The points connected by solid lines represent viscoelastic systems 2V–5V. The unconnected points correspond to Newtonian systems 5 and 6.

$\Delta P^+$ on the size of the drop is not qualitatively changed by variations in eccentricity (i.e. $\Delta\rho/\rho_0$) for a Newtonian suspending fluid. Thus, although the majority of Newtonian systems in table 3 show a monotonic increase in $\Delta P^+ R_0/\mu_0 V$ with drop size, the previous work on neutrally buoyant drops shows clearly that this behaviour depends upon the value of $\sigma$. In particular, for $\sigma$ small enough and $\lambda$ large enough, the extra pressure difference must decrease with increased drop size, for the simple reason that fluid of higher viscosity is being replaced by fluid of lower viscosity. The fact that $\Delta P^+ R_0/\mu_0 V$ increases with drop size in all cases shown in figure 4 is a consequence of the fact that the minimum value of $\sigma$ was only 0·3, and the maximum in $\lambda$ was 0·83. Indeed, the system 4 (see table 3) illustrates a partial transition to the small-$\sigma$, large-$\lambda$ behaviour noted in Ho & Leal (1975). This system has the lowest viscosity ratio ($\sigma = 0{\cdot}30$) of those studied here, and the additional pressure difference first increases with $\lambda$ in this particular system, achieves a maximum around $\lambda \simeq 0{\cdot}6$ (for $V = 0{\cdot}80$ cm/s), and then decreases as the size of the drop is made larger. The important inference is that simple fluid replacement must eventually establish the large-$\lambda$ behaviour for $\Delta P^+$ regardless of the additional mechanisms that are significant for smaller drop sizes. The magnitude of $\Delta P^+$ will then depend mainly on the value of $\sigma$. Further support for this view comes from the fact that $\Delta P^+$ increases with $\lambda$ at a rate which, for the largest values of $\lambda$, appears to be independent of the drop eccentricity, as would in fact be expected when the dominant mechanism is simple fluid replacement.

In contrast to the effect on $\Delta P^+$, the qualitative dependence of the relative velocity of the drop on drop size does depend on the eccentricity of the drop for Newtonian

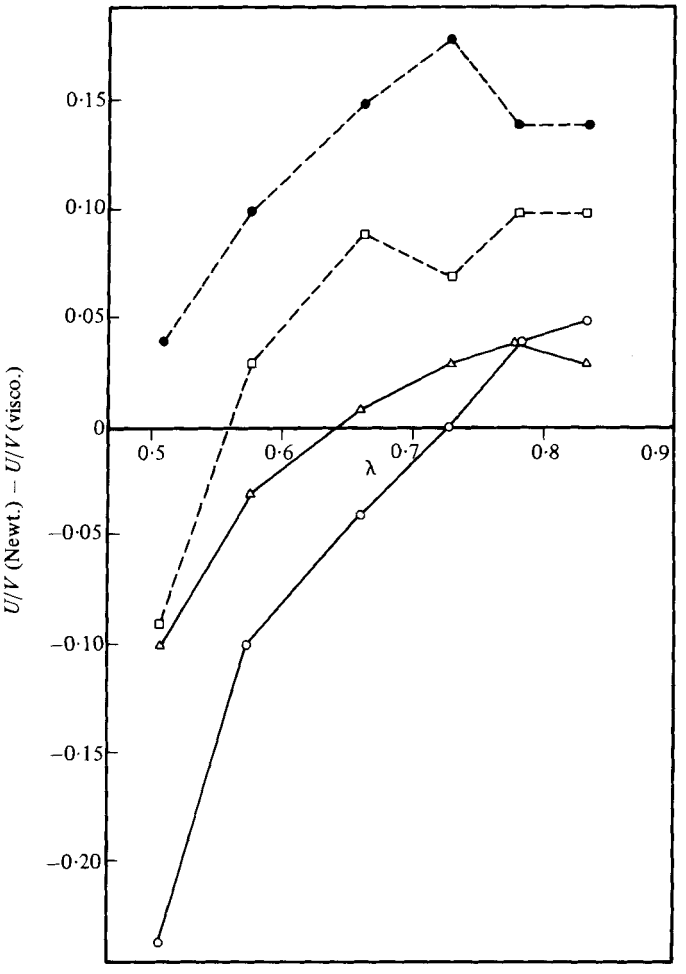


FIGURE 6. Difference between $U/V$ for Newtonian and viscoelastic suspending fluids as a function of drop size. ●, $U/V$ (system 2) − $U/V$ (system 6V), $V = 0{\cdot}56$ cm/s; □, $U/V$ (system 2) − $U/V$ (system 6V), $V = 0{\cdot}32$ cm/s; △, $U/V$ (system 6) − $U/V$ (system 2V) $V = 0{\cdot}56$ cm/s; ○, $U/V$ (system 6) − $U/V$ (system 2V), $V = 0{\cdot}32$ cm/s.

suspending fluids. It was shown in Ho & Leal (1975) that the velocity ratio $U/V$ for a neutrally buoyant drop decreases monotonically with increasing $\lambda$ until a constant limiting value is attained around $\lambda \simeq 0{\cdot}9$. The least non-neutrally buoyant drops studied here, system 4 ($\Delta\rho/\rho_0 = 0{\cdot}011$), also show a monotonic decrease in $U/V$ up to $\lambda = 0{\cdot}83$, which was the largest value covered in this study. However, for the other non-neutrally buoyant systems ($\Delta\rho/\rho_0 = 0{\cdot}02$, $0{\cdot}04$), $U/V$ first increases with $\lambda$, attains a maximum around $\lambda \simeq 0{\cdot}6$–$0{\cdot}7$, and then decreases monotonically with further increase in $\lambda$.

Finally, it can be seen from figure 5 that the drop undergoes larger shape deformations in Newtonian systems as its size (i.e. $\lambda$) is increased. In contrast to this, the relative degree of deformation in an unbounded creeping flow would be independent of the drop size. However, in the present case, the drop is deformed, in part, due to the presence of the walls, and it is this effect which is responsible for the observed increase in deformation with larger $\lambda$.

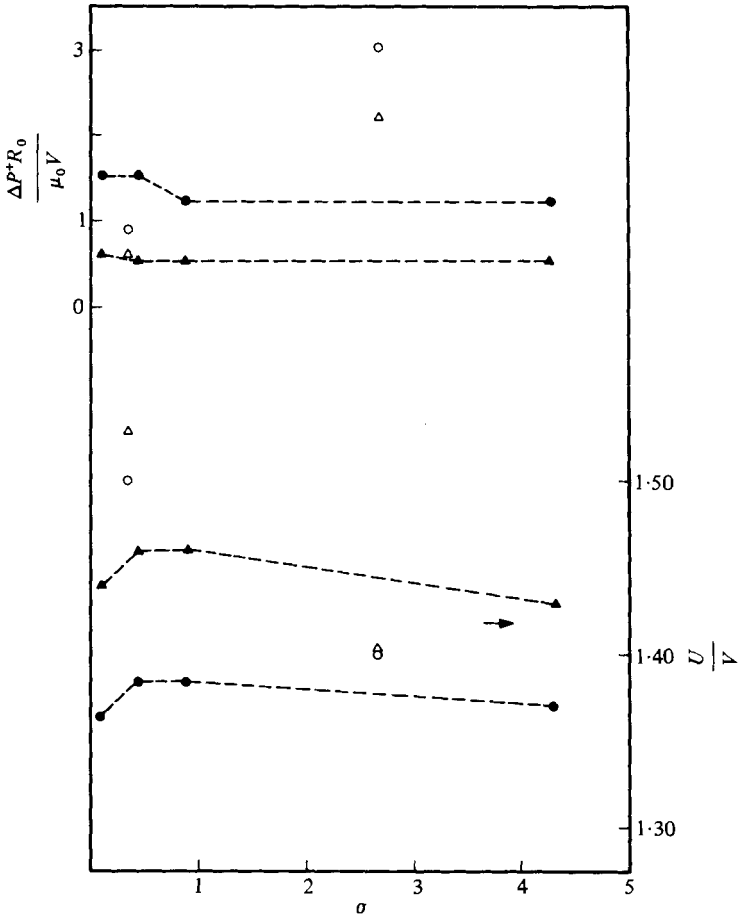


FIGURE 7. Dimensionless extra pressure difference and relative velocity of drop as functions of viscosity ratio for $V = 0{\cdot}56$ cm/s, $\Delta\rho/\rho_0 = 0{\cdot}04$. Newtonian systems 5 and 6: △, $\lambda = 0{\cdot}576$; ○, 0·726. Viscoelastic systems 2V–3V: ▲, $\lambda = 0{\cdot}576$; ●, 0·726.

*Viscoelastic suspending fluid.* The qualitative dependence of $\Delta P^+$ on $\lambda$ for viscoelastic suspending fluids is clearly similar (see figure 4) to its dependence for the Newtonian systems – namely, an increase in $\Delta P^+$ is observed with any increase in $\lambda$. What is *different*, however, is the fact that both the rate of increase and the actual non-dimensionalized values of $\Delta P^+ R_0/\mu_0 V$ are apparently independent of all the material parameters in the viscoelastic case, including $\sigma$ (cf. figure 4). Furthermore, no maximum or asymptotic limit is observed for $\Delta P^+ R_0/\mu_0 V$ over the size range covered.

Another contrast between Newtonian and viscoelastic suspending fluids is the absence of a maximum in $U/V$ as a function of $\lambda$ (table 3) for any $\Delta\rho/\rho_0$ that we considered. Instead, $U/V$ only decreases monotonically with increasing drop size at a rate which again seems to be independent of other material parameters, including $\sigma$. The *relative* mobility of drops in viscoelastic and Newtonian systems depends on drop size. A comparison between various Newtonian and viscoelastic systems shows that $U/V$ is often larger in the viscoelastic systems for small drops, but is always

smaller for large drops in the size range covered here. Typical curves for the *difference* between $U/V$ for the Newtonian systems and $U/V$ for a corresponding viscoelastic system (same $\Delta\rho/\rho_0$, $\sigma$) are shown in figure 6 as a function of $\lambda$.

### 3.3. *Drop viscosity*

The effect of drop viscosity relative to the viscosity of the suspending fluid was studied by taking measurements for various grades of drop fluid at each value of $\Delta\rho$ ($\sim 0{\cdot}1 < \sigma < \sim 5$). The results are shown in figures 3, 5 and 7, as well as table 3.

*Newtonian suspending fluid.* In the case of Newtonian fluid systems, $\Delta P^{+}R_0/\mu_0 V$ increases with increase of $\sigma$, as can be seen from figure 7, while the drop velocity decreases (cf. figure 7) and the drop deformation, as measured by $D$, increases very slightly (cf. figure 5). The drop viscosity does *not*, however, affect the gap width between the drop and the tube wall over the entire range of experimental conditions of this study. Although the decrease in drop velocity with increase of $\sigma$ is predicted qualitatively by (1) for undeformed drops, the Newtonian results from table 3 show that the drop velocity is more sensitive to $\sigma$ for more eccentric drops and this feature cannot be predicted by the small-$\lambda$, spherical drop theory. The fact that drop deformation is relatively insensitive to the drop viscosity is qualitatively consistent with the results of Taylor (1932) and others for drop deformation in a simple shear flow of an unbounded fluid.

*Viscoelastic fluid systems.* The qualitative effects of the viscosity ratio $\sigma$ are very different in the case of a viscoelastic suspending fluid. Firstly, figure 7 shows clearly that, for eccentric drops, the additional pressure difference is independent of the value of $\sigma$ over the range of $\sigma$ studied, in marked contrast to the Newtonian result. Secondly, the drop velocity is very nearly independent of $\sigma$. The gap width and drop shape are also essentially independent of $\sigma$, but this is the same result as for a Newtonian fluid. It may be noted that the additional pressure difference is positive for all cases studied, even for viscosity ratios as low as $\sigma = 0{\cdot}09$. Furthermore, $\Delta P^{+}R_0/\mu_0 V$ is larger for viscous drops in a Newtonian suspending fluid than for the same drops in a viscoelastic system, if all other parameters remain unchanged. The opposite is found for inviscid drops.

### 3.4. *Density difference*

Finally, let us consider the effects of the eccentric position of non-neutrally buoyant drops. The equilibrium position of a non-neutrally buoyant drop is determined by a balance between buoyancy forces and hydrodynamic lift generated in the gap between the drop and the tube wall. The value of $\Delta\rho/\rho_0$ ranges from zero in Ho & Leal (1975) to 0·04 in the present study.

*Newtonian suspending fluid.* The dependence of $\Delta P^{+}R_0/\mu_0 V$ and $U/V$ on the density difference $\Delta\rho/\rho_0$ is illustrated in figure 8. Clearly, the additional pressure difference increases for a Newtonian suspending fluid as a drop of fixed size is made more eccentric by increasing the drop density. Also, the velocity of the drop decreases, and the drop suffers a larger deformation. Surprisingly, the sensitivity of $\Delta P^{+}R_0/\mu_0 V$ to variations in $\Delta\rho/\rho_0$ diminishes above $\Delta\rho/\rho_0 = 0{\cdot}02$ for the drops with $\lambda = 0{\cdot}83$. In contrast, smaller drops show an appreciable increase in $\Delta P^{+}R_0/\mu_0 V$ with $\Delta\rho/\rho_0$ up to $\Delta\rho/\rho_0 = 0{\cdot}04$. Small drops also show a much stronger dependence of $U/V$ on

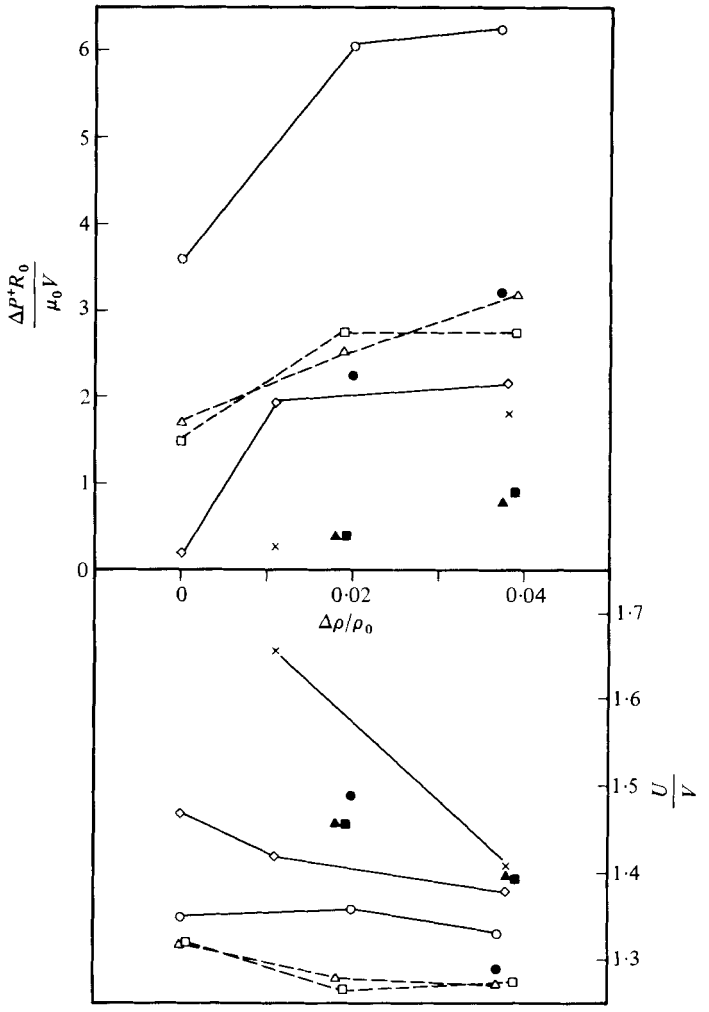


FIGURE 8. Dimensionless pressure difference and relative velocity as functions of $\Delta\rho/\rho_0$. Newtonian systems 4 and 5: ×, $\lambda$ = 0·660; ◇, 0·831. Newtonian systems 2 and 6: ●, $\lambda$ = 0·660; ○, 0·831. Viscoelastic systems 2V and 6V: ■, $\lambda$ = 0·660; □, 0·831. Viscoelastic systems 4V and 8V: ▲, $\lambda$ = 0·660; △, 0·831. All data for $V$ = 0·32 cm/s. Also shown are results from Ho & Leal (1975) for $\Delta\rho/\rho_0$ = 0.

$\Delta\rho/\rho_0$ than the corresponding large drops. However, the most significant result is the extreme sensitivity of the data to $\Delta\rho/\rho_0$.

*Viscoelastic suspending fluid.* The same qualitative trends noted above for Newtonian systems were also observed for viscoelastic suspending fluids, though the effects are less pronounced.

A key difference between the two cases, however, is the gap width $h$. For a given value of $\Delta\rho/\rho_0$, drops suspended in a viscoelastic fluid are much farther from the wall than those in a Newtonian fluid. For example, the values of $h$ for two corresponding viscoelastic and Newtonian systems, with $\Delta\rho/\rho_0$ = 0·019, are 0·32 (system 6V) and 0·12 (system 2) for $\lambda$ = 0·62, and 0·18 (system 6V) and 0·12 (system 2) for $\lambda$ = 0·83.

Comparison between the results obtained here and those in Ho & Leal for neutrally

buoyant drops shows that the effects of a given magnitude of $\Delta\rho/\rho_0$ on the drop eccentricity decreases as the size of the drop is made larger. Consequently, a given value for $\Delta\rho/\rho_0$ induces a relatively smaller change in the measured quantities as the drop is made larger.

## 4. Further discussion

### 4.1. *Relevance of lubrication ideas*

Photographs of the non-neutrally buoyant drops in flow suggest that the fluid-filled gap between the drop's lower surface and the tube wall is a lubrication layer capable of producing an upward thrust on the drop which balances buoyancy. It is essential, then, that the drop is able to deform in the flow, since a spherical drop can generate no hydrodynamic lift in a Newtonian fluid at small Reynolds number. Indeed, the lateral position of an *undeformed* neutrally buoyant drop is determined exclusively by its initial lateral position in the tube, provided the Reynolds number and Deborah number are sufficiently small that 'lateral migration effects' are negligible (cf. Chan & Leal 1979). It is the lack of an inherently preferred radial position for a spherical drop which is responsible for the extreme sensitivity of the measured results to small variations in $\Delta\rho/\rho_0$.

For non-neutrally buoyant deformable drops, previous lubrication analyses of related flows may be useful. The most relevant study is by Lighthill (1968), who considered the motion of an elastic particle through a capillary in a Newtonian suspending fluid. The particle is assumed to be neutrally buoyant and close-fitting, but capable of deforming to 'squeeze through' the tube. Lighthill applied classical lubrication theory to determine the flow field in the gap between the particle and the wall. The results predict that both the thickness of the lubrication layer and the additional pressure difference should vary proportionally to $U^{\frac{1}{2}}$.

The qualitative relevance of Lighthill's analysis for non-neutrally buoyant viscous drops is tested in figure 9. Each point for the Newtonian systems actually represents an average value for $h^2$ over all drop sizes for each choice of drop fluid and $V$, since it was previously found for Newtonian systems that there is no measurable variation of $h$ with $\lambda$ for sufficiently large values of $\Delta\rho/\rho_0$ where the lubrication approximation is most likely to be valid. In the viscoelastic systems, $h$ varies with $\lambda$ and in these cases only the values of $h$ for the largest drops were used in figure 9. The existence of a linear relationship between $h^2$ and $U/\Delta\rho$ suggests that, indeed, the velocity of the particle and gap width are determined by forces generated in a lubrication layer, albeit one which acts on only one 'side' of the drop, since the particles in the present study are neither concentric nor close-fitting. The analysis of Lighthill applies to solid elastic particles, and the data for the Newtonian cases shown in figure 9 exhibits a slight dependence on the drop viscosity, especially near the origin. The coefficient of proportionality for the lubrication correlation between $h^2$ and $U$ appears to be larger for smaller values of $\sigma$ for the Newtonian suspending fluid. Indeed, when the lubrication analysis is modified to account for the fact that the particle is a liquid drop, it can be shown that the gap thickness $h$ remains dependent on $U^{\frac{1}{2}}$ (even as $\sigma \to 0$), but the constant of proportionality increases by a factor of two as $\sigma$ decreases from infinity to zero.

The pressure generated in the lubrication layer which balances the non-neutral

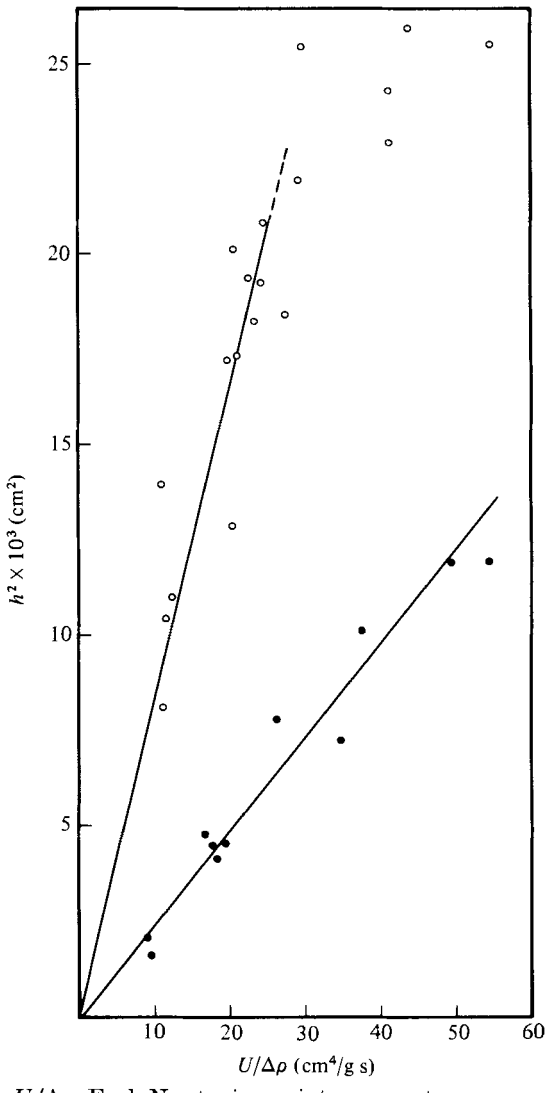


FIGURE 9. $h^2$ versus $U/\Delta\rho$. Each Newtonian point represents an average of all drop sizes for the particular system and flow rate. The viscoelastic points are taken for the largest drop sizes. Suspending fluid: ●, 95·75% glycerine; ○, 0·5% Separan.

buoyancy of the drop is proportional to $\mu_0 U/h^2$ for any value of $\sigma$. Thus, we expect that the effect of an increase in the viscosity of the suspending fluid will be a greater gap thickness for a fixed value of $\Delta\rho/\rho_0$. The values of $h^2$ and hence the slopes of the two lines which approximate the Newtonian and viscoelastic data shown in figure 9 should therefore be related to the viscosities of the suspending fluids. Since little or no variation could be discerned in the coefficient of proportionality with changes in $\sigma$, we have approximated each set of data by a single curve. The viscosity of the Newtonian solution, 95·75% aqueous glycerin, was determined to be 4·17 P. The viscosity of the shear-thinning 0·5% Separan solution depends strongly, of course, on the flow rate. However, for sufficiently small values of $V$ (and $U$), the viscosity is

just the zero-shear-rate viscosity which we have estimated from viscometric data to be approx. 14·5 P. Thus, the ratio of slopes in figure 9 for small values of $U$ (i.e. near the origin) is expected to be $14{\cdot}5/4{\cdot}17 = 3{\cdot}5$. This agrees well with the actual ratio of 3·1.

It is surprising, however, that the linear relationship between $U$ and $h^2$ holds for the viscoelastic case over a wide range of flow rates. The effective viscosity of the suspending fluid, which can be deduced from table 1, decreases by as much as 50 % based on the wall shear rate as the flow rate increases over the range covered in figure 9. We would expect, on the basis of the dependence of $h^2$ on $\mu_0$ alone, that $h^2$ should decrease by as much as 50 % from its 'zero-shear-rate' value owing to shear-thinning. Instead, there appears to be no effect of the variations in the suspending-fluid viscosity that are associated with increases in shear rate. We believe that the explanation for this involves the normal stresses which are present in the viscoelastic suspending fluid. The primary normal-stress difference gives rise to a hoop stress by creating a tension in the curved streamlines around the drop. This tension in the streamlines is greatest at the location of greatest shear rate, which is clearly in the gap between the particle and the tube wall. The net effect of normal-stress-induced hoop stresses is thus to 'push' the particle away from the tube wall, toward the centre line. Now the magnitude of the primary normal-stress difference for 0·5 % Separan AP-30 increases approximately as the square of the shear rate in the range of interest (Leal *et al.* 1971), while the viscosity of 0·5 % Separan AP-30 decreases approximately as the square of the shear rate. Thus, as $U$ is made larger, the potential increase in $h^2$ from the increased hoop thrust and the decrease in $h^2$ which is caused by the decrease in suspending fluid viscosity tend to balance one another. An apparent consequence of this off-setting effect is that the qualitative variation of $h^2$ with $U$ is not changed in a viscoelastic fluid from the Newtonian lubrication result.

The lubrication analysis for a solid particle predicts also that the additional pressure difference $\Delta P^+$ should vary with $U^{\frac{1}{2}}$. This result depends crucially on the axial force on the lubrication surface which, in turn, depends on the shear stress at the particle surface. When the particle is a drop, the appropriate boundary condition at the particle surface is continuity of stress and velocity rather than the no-slip condition which is appropriate for a solid particle. We expect, then, that $\Delta P^+$ will scale with $U^{\frac{1}{2}}$ only for 'highly viscous' drops. Data from table 3 show that this is the case. For the more viscous drops, system 2 and system 6 ($\sigma = 2{\cdot}63$ and 2·68, respectively), the measured values for $\Delta P^+$ scale (to within 20 %) with $U^{\frac{1}{2}}$. Furthermore, when the lubrication approximation is written for a shear-thinning fluid using a power-law model, it can be shown that $\Delta P^+$ should vary with $U^{n/(n+1)}$, where $n$ is the power-law index. Thus, for fluids with $n < 1$, $\Delta P^+$ should be less sensitive to $U$ than for a Newtonian fluid ($n = 1$). Indeed, the data for $\Delta P^+$ from table 3 for viscous drops suspended in 0·5 % Separan (systems 2V and 5V) scale with $U^{0{\cdot}31}$ (to within 20 %), where the exponent corresponds to $n = 0{\cdot}45$ (see § 2).

The lubrication model also provides a useful qualitative explanation of the fact, noted in § 3, that $\Delta P^+$ becomes relatively independent of $\Delta\rho/\rho$ for large drops, once $\Delta\rho/\rho_0$ exceeds about 0·02. From the point of view of lubrication theory, as the gap becomes smaller it takes smaller decreases in the gap width to yield a given incremental increase in the hydrodynamic lift. This reflects the fact that pressures in the lubrication layer scale with $1/h^2$. Thus, as $\Delta\rho/\rho_0$ is made larger, the variation in $h$ which is required to balance drop buoyancy becomes smaller, and quantities such as

$\Delta P^+$, which are less sensitive to $h$ than the lubrication pressure, will tend to become insensitive to further increases in $\Delta\rho/\rho_0$. It may be noted, in this regard, that the lubrication analysis predicts that $\Delta P^+$ varies only as $1/h$. Since it would take an infinite value of $\Delta\rho$, from the strict viewpoint of lubrication theory, to reduce the gap width $h$ to zero, it is obvious that $\partial h/\partial(\Delta\rho)$ must decrease as $\Delta\rho$ increases. This is exactly what was observed. Further, since $h$ will be smaller for a larger drop (other factors such as $\Delta\rho$ being equal), larger drops should be expected to display asymptotic behaviour for lower values of $\Delta\rho/\rho_0$. The small drops, too, will become less sensitive to $\Delta\rho$, but only at larger values of $\Delta\rho/\rho_0$, apparently outside the range of this study.

We have already noted that drop deformation is essential to the generation of hydrodynamic lift via the lubrication mechanism. This would suggest that the results for $\Delta P^+$ and $U/V$ should show a dependence on the degree of deformation induced by the flow. Indeed, the theoretical analyses of Hyman & Skalak (1972*b*) and Fitz-Gerald (1969) suggest that any factor which causes increased drop deformation will result in a simultaneous increase in the drop's relative velocity and a decrease in the additional pressure drop. The data for both the Newtonian and viscoelastic systems studied here tend to confirm these implications of the available theories in the sense that an increase in the value of the deformation parameter $\Gamma$ was found to lead to increased deformation, increased mobility and a decreased additional pressure drop.

### 4.2. *The influence of viscoelasticity*

We have previously discussed certain consequences of viscoelasticity in the suspending fluid, particularly in the framework of the lubrication ideas of §4.1. Here, we focus on other aspects of the influence of viscoelasticity, starting with the observations described in §3 of $\Delta P^+$ for viscoelastic suspending fluids.

The primary distinction between the data for $\Delta P^+ R_0/\mu_0 V$ in viscoelastic and Newtonian fluid systems is that the latter show increased values of $\Delta P^+ R_0/\mu_0 V$ with increased values of $\sigma$, while $\Delta P^+ R_0/\mu_0 V$ in the viscoelastic case is virtually independent of the drop viscosity. In part, this latter result must be a consequence of the limited range of values for $\lambda$ covered by the experiments, for it was shown in Ho & Leal (1975) that $\Delta P^+ R_0/\mu_0 V$ for neutrally buoyant drops is dominated by the simple fluid-replacement mechanism for sufficiently large drops, even in viscoelastic systems, so that the *sign* of $\Delta P^+$ must eventually depend upon whether $\sigma$ is smaller or larger than unity. This does not, of course, address the question as to why $\Delta P^+ R_0/\mu_0 V$ should be independent of $\sigma$ for smaller values of $\lambda$ in the case of a viscoelastic suspending fluid. One *possibility* is that the behaviour of smaller drops is dominated by elastic properties of the suspending fluid rather than the shear viscosity which is used to correlate the data for large drops. Now, the Deborah number for the flow (see §2) is approximately

$$De = \frac{(U-V)\theta}{2D\lambda R_0},$$

where $2D\lambda R_0$ is the 'length' of the deformed drop, $U-V$ is the difference between the drop velocity and the suspending-fluid average velocity, and $\theta$ is the fluid relaxation time. The present data for a viscoelastic suspending fluid show that, as $\lambda$ is increased, $D$ increases and $U$ tends toward $V$ (i.e. $U/V$ decreases monotonically). Thus, in the range of $\lambda$ covered here, the effect of increasing $\lambda$ is to *decrease* the value

of $De$. This indicates that elastic effects should be more significant for the smaller values of $\lambda$. This reasoning cannot hold, of course, as $\lambda \to 0$, since in this limit the particle velocity tends toward the local velocity of the suspending fluid with $\lambda^2$ dependence, and hence $De \to 0$. We conclude that elastic effects will be most significant for smaller but non-zero values of $\lambda$, and it is possible that $De$ becomes sufficiently large in this range for the onset of dominant elastic behaviour in the suspending fluid which could render $\sigma$ relatively unimportant. It should be noted, however, that the largest value of $De$ estimated for the conditions of the present experiments is only 0·20, and it is usually held that strong elastic effects are not observed until $De$ is increased to a value of 1 or 2. In point of fact, the 'onset' value of $De$ for a given experiment can only be verified by a systematic variation of the fluid response time, which was not done in the present study. The idea that dominant fluid elasticity may be responsible for the observed insensitivity to $\sigma$ for smaller values of $\lambda$ must therefore be regarded as speculative. We may, however, mention that results from related experiments by Sigli & Coutanceau (1977) on a *rigid* sphere ($0{\cdot}25 \leqslant \lambda \leqslant 0{\cdot}75$) sedimenting in a vertical cylindrical tube are at least qualitatively consistent with the suggestion of dominant elasticity for relatively small values of $De$. In that case, fluid elasticity was found to have a strong effect on the drag on the sphere for values of the Deborah number $\theta V_0/R_0$, where $V_0$ is the terminal velocity of the sphere, as low as 0·05. Sigli & Coutanceau speculated that the importance of elasticity in the suspending fluid was somehow enhanced by the presence of the tube wall.

It is noteworthy that $\Delta P^+ R_0/\mu_0 V$ (and $\Delta P^+$ itself) in the viscoelastic suspending fluid falls well below the Newtonian values, for approximately equal values of $\sigma$, $\lambda$ and $\Delta\rho/\rho_0$. The complete quantitative significance of this observation is difficult to assess, because the dimensionless values plotted in figure 3 for the viscoelastic fluids use the viscosity evaluated at the wall shear rate. Since this is the highest shear rate in the flow, the value of $\mu_0$ used in figure 3 is the minimum possible value for the particular undisturbed flow conditions, and thus $\Delta P^+ R_0/\mu_0 V$ (as plotted) is the *maximum* value which could have been assigned to the viscoelastic data for a given $\Delta P^+$, $R_0$ and $V$. Regardless of these details, however, the dimensionless extra pressure difference in figure 3 shows similar dependence on $\Gamma$ for both suspending fluids. It thus appears that the data correlate without need for explicit consideration of the Deborah number, or any other viscoelastic parameter which depends, in principle, on $V$. This seems to contradict our speculation that $\Delta P^+$ may be independent of $\sigma$ for smaller drops owing to dominant elastic effects in the suspending fluid. However, the data of Sigli & Coutanceau (1977) suggest another possible explanation for our results. Their results show that the drag on a rigid sphere moving through a viscoelastic fluid in a circular tube ($0{\cdot}25 \leqslant \lambda \leqslant 0{\cdot}75$) is considerably smaller than the drag on the same sphere in a Newtonian fluid, even after the viscosity is adjusted for the effects of shear-thinning. The decrease in the relative drag takes place completely as $\theta V_0/R_0$ is increased from zero (Newtonian) to approximately 0·5 for $\lambda = 0{\cdot}5$. For values of $\theta V_0/R_0 > 0{\cdot}5$, the *relative* drag is nearly independent of $De$ and, in this regime of $De$, the drag shows the same qualitative dependence on $V_0$ in both Newtonian and viscoelastic suspending fluids, even though the magnitude of the drag is smaller in the viscoelastic fluid. The implications of these results are that elastic effects are observed at values of $De$ considerably smaller than usually expected, and that these effects may become *asymptotic* in $De$ at relatively small values of $De$.

### 4.3. *The effect of the undisturbed flow profile on drop mobility*

The data for the *relative velocity* of the drop show a maximum at intermediate $\lambda$ for some drops in a Newtonian suspending fluid. This suggests that drop mobility, like $\Delta P^+$, is determined by competitive effects. Existing theoretical calculations for *small* $\lambda$ suggest that there are two primary factors which determine the velocity of eccentric drops in a Newtonian fluid. First, there is the hydrodynamically induced slip velocity, which causes the drop to move at a velocity less than the undisturbed velocity of the surrounding fluid. Secondly, the drops move at a velocity that reflects the undisturbed fluid velocity at the radial position occupied by their centre point, and the undisturbed velocity varies relative to the mean, as a function of radial position. The drops in the present study are not 'small' but, still, the velocities of the undisturbed path lines 'occupied' by the drop apparently remain significant for the determination of the drop velocity at intermediate values of $\lambda$, and it is this fact which we believe accounts for the qualitative changes in $U/V$ as a function of $\lambda$ as the density difference, $\Delta\rho/\rho_0$, is increased.

When $\Delta\rho/\rho_0$ is small, the gap between the drop and the tube wall decreases as the drop is made larger and, though the centre of the drop remains near the centre of the tube, it gradually moves outward toward the wall, thus occupying undisturbed streamlines with velocities lower, on average, than those closer to the centre line. For example, Newtonian system 4 exhibits a monotonic decrease in $h$ from 0·40 for $\lambda = 0{\cdot}51$ to 0·16 for $\lambda = 0{\cdot}87$, for $V = 0{\cdot}56$ cm/s (see table 1), and $U/V$ is expected, as a consequence, also to decrease monotonically as it is, in fact, observed to do. On the other hand, higher-density drops show comparatively little effect of $\lambda$ on $h$. For Newtonian system 6, for example, $h$ varies only between 0·12 and 0·14 over the entire range of drop sizes. Since the data show that gap width does not change with size, the centre of the smallest drop must be situated closer to the tube wall than the centre of a larger drop in this case. Thus, as the size of the drop increases in a Newtonian suspending fluid, the centre of the drop 'moves' toward the tube centre line, and the drop occupies more of the region of greater undisturbed velocities. As a result, the drop is observed to move with a *greater* relative velocity in the Newtonian suspending fluid as $\lambda$ is increased for moderate values of $\lambda$. However, the drop exhibits a *maximum* velocity around $\lambda \simeq 0{\cdot}7$ for all Newtonian systems except system 4. For large drops with values of $\lambda > 0{\cdot}7$, the drop nearly fills the tube, and wall interactions, which tend to retard the motion of the drop, apparently become more significant, as in the neutrally buoyant case. Thus, $U/V$ decreases with further increase in $\lambda$ until $\lambda \to 1$. Then, $U/V$ remains constant with increasing $\lambda$ since further increases in volume lead to increases in drop length rather than changes in its cross-section (cf. Ho & Leal 1975).

In contrast to the Newtonian case, $U/V$ is a monotonically decreasing function of $\lambda$ for all of the viscoelastic suspending fluid systems which we studied. Once again, this result appears to be correlated with the relationship between $\lambda$ and the gap width $h$. We have already noted that $h$ is significantly larger for the viscoelastic suspending fluids than for the Newtonian fluids. This difference is greater for smaller drops and lower flow rates. In addition, the viscoelastic systems show a monotonic decrease in the gap width as the size of the drop increases for all flow rates. Thus, the behaviour for the viscoelastic systems is qualitatively similar to the Newtonian system 4, the least non-neutrally buoyant case in the present study.

The suggestion that drop mobility depends, at least in part, on the undisturbed pathlines sampled by the drop also helps to explain the results of figure 6, which show that $U/V$ is often larger for small drops in the viscoelastic systems compared to the Newtonian cases, but never larger for large drops. If a power-law model with index $n = 0{\cdot}45$ (see §2) is used to describe the suspending fluid, the undisturbed velocity profile is considerably blunted near the centre of the tube. The maximum velocity on the centre-line is less than the Newtonian case, only $1{\cdot}6V$. For a fixed-volume flow rate, the Newtonian fluid exhibits larger velocities than the viscoelastic fluid for dimensionless distances from the tube centre line, $\beta$, up to $\beta = 0{\cdot}6$. From $\beta = 0{\cdot}6$ to $\beta = 1{\cdot}0$ (the tube wall), on the other hand, the power-law fluid exhibits the greater velocities. Since the relative velocity of the drop depends in part on the velocity of the undisturbed streamlines occupied by the drop, it follows that small, highly eccentric drops which occupy the region adjacent to the wall should move more rapidly in a power-law fluid than in a Newtonian fluid (because the shear-thinning fluid itself is moving faster). Thus, it is clear that the mobility of *small* non-neutrally buoyant drops is favoured for a shear-thinning fluid, at least insofar as the undisturbed profiles are concerned. The data from the present experiments show that increased values of $\Delta\rho/\rho_0$ and decreased values of $V$ (for $\Delta\rho/\rho_0 \neq 0$) alone or together, cause the drop to assume a more eccentric position in the tube. Figure 6 shows that $U/V$ (Newtonian) $- U/V$ (viscoelastic) is more negative for smaller values of $V$ and for larger values of $\Delta\rho/\rho_0$. This is in accord with the simple mechanism proposed above. As a small drop is made larger, however, more of the centre of the tube is occupied by the drop, i.e. $\beta$ decreases, and the drop becomes less eccentric. The undisturbed velocity in this region is not only greater than that near the tube wall, but is also relatively greater for the Newtonian suspending fluid than for the viscoelastic fluid. Thus, as $\lambda$ is made larger, it may be expected that the mobility of drops will ultimately be favoured for the Newtonian suspending fluid.

## 5. Comparison with theory

Our discussion of the experimental results has focused until now on a description of the qualitative effects of the various independent variables on the measured quantities. Now, a comparison between the data for Newtonian fluid systems and the available theoretical calculations for $\Delta P^+$ and $U$ in a Newtonian fluid will, it is hoped, provide additional insight into the various physical phenomena involved and test the range of applicability of the analyses. It should be remembered, in making such a comparison, that the analytical theories leading to (1) and (2) are restricted to small drops, $\lambda \ll 1$, which have spherical shapes and to a Newtonian suspending fluid. Furthermore, there is no consideration of wall effects, except insofar as the bounding wall gives rise to the undisturbed Poiseuille flow.

No theory presently exists for predicting the position of the drop relative to the wall, i.e. $\beta$ which appears in (1) and (2). Consequently, (1) is not capable of *a priori* predictions for the qualitative trends displayed by the data – the variation of $U/V$ with $V$, for example. However, $\beta$ can be measured from photographs and then used in (1) to evaluate $U/V$ for quantitative comparison with the data.

Figure 10 shows $U/V$ as a function of $\lambda$ for two systems selected to illustrate the effect of $\sigma$. Equation (1), using the appropriate measured value for $\beta$ for each case,

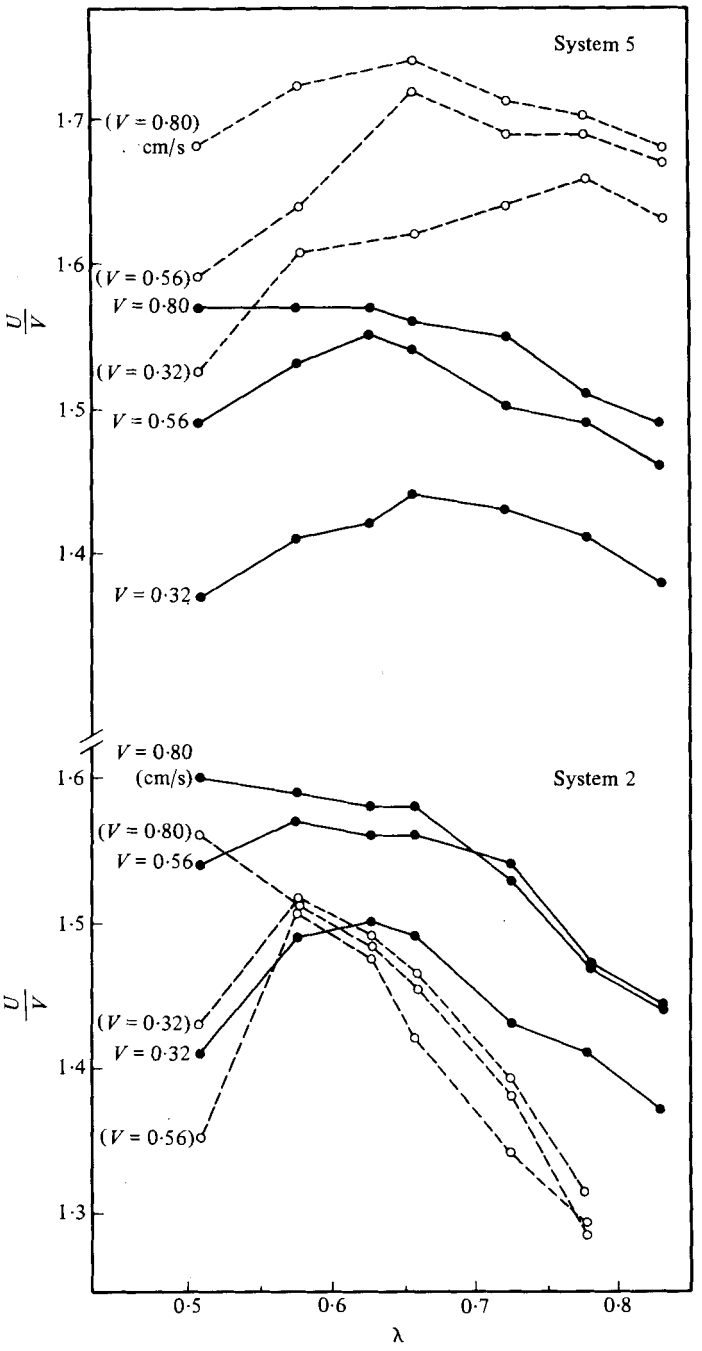


FIGURE 10. Data for relative drop velocity as a function of dimensionless drop size. ●, systems 2 and 5 (Newtonian). ○, predicted values from (1).

| Viscosity ratio | Coefficients of (2): Concentric ($\lambda^5$) term | Eccentric ($\beta^2\lambda^3$) term |
|---|---|---|
| 0·30 | −2·82 | 28·72 |
| 0·35 | −1·94 | 29·63 |
| 0·77 | 3·09 | 35·25 |
| 2·63 | 10·22 | 44·52 |
| 2·68 | 10·30 | 44·64 |

TABLE 4. Coefficients of equation (2)

is compared to the data. Qualitative agreement between the two is good, inasmuch as a maximum value for $U/V$ at intermediate $\lambda$ is predicted only for the systems which actually show one. Otherwise, (1) predicts a monotonic decrease in $U/V$ as $\lambda$ is made larger. It may be noted that the maximum in $U/V$ actually results from a minimum in the experimentally observed values of $\beta$ as a function of $\lambda$. Furthermore, quantitative comparison between the data and (1) shows that the effect of $\sigma$ on $U/V$ is not as significant as indicated by the slip-velocity term.

The only means by which (1) predicts any variation in $U/V$ with $V$ is through the measured value of $\beta$. Figure 10 shows that the variation in $U/V$ with $V$ is not predicted adequately by (1). An effect not taken into account in the derivation of (1) is the deformed shape of the drop. It has already been suggested that deformation is partly responsible for the observed increase in $U/V$ with $V$, but the theory which leads to (1) predicts that the deformation of the drop should be unimportant if

$$\frac{\mu_0 V\lambda\beta}{\gamma} \ll 1.$$

The value of the left-hand side of the inequality never exceeds 0·06 for the range of material parameters used in the present study, indicating that drop deformation should be insignificant. Nevertheless, the photographs show that the drop undergoes appreciable deformation, and the data show a dependence on the degree of deformation, as already outlined in § 3. A mechanism that could induce increased deformation which is not included in the theoretical analysis is the hydrodynamic interaction between the drop and the wall.

Equation (2) for the additional pressure difference contains one term for the concentric contribution and another for the effect of non-neutral buoyancy. The neutrally buoyant term depends on $\lambda^5$ while the non-neutrally buoyant one contains $\beta^2\lambda^3$. Table 4 shows the magnitude of these terms, relative to each other, at the values of $\sigma$ used in the present experiment.

The predicted contribution due to drop eccentricity is always positive and only weakly dependent on the viscosity of the drop. The concentric term, which includes the contribution due to the replacement of fluid, can be positive or negative, depending on the viscosity ratio, but is always considerably smaller in magnitude than the eccentric term. The effect of drop eccentricity is always to increase $\Delta P^+$ over the neutrally buoyant case. The value of $\sigma$ where $\Delta P^+ = 0$ is predicted to depend on $\beta^2/\lambda^2$, decreasing from $\sigma = 0{\cdot}48$ for $\beta^2/\lambda^2 = 0$ to $\sigma = 0$ for $\beta^2/\lambda^2 = 0{\cdot}5$.

Once again, $\beta$ must be evaluated from photographs of the drops for quantitative

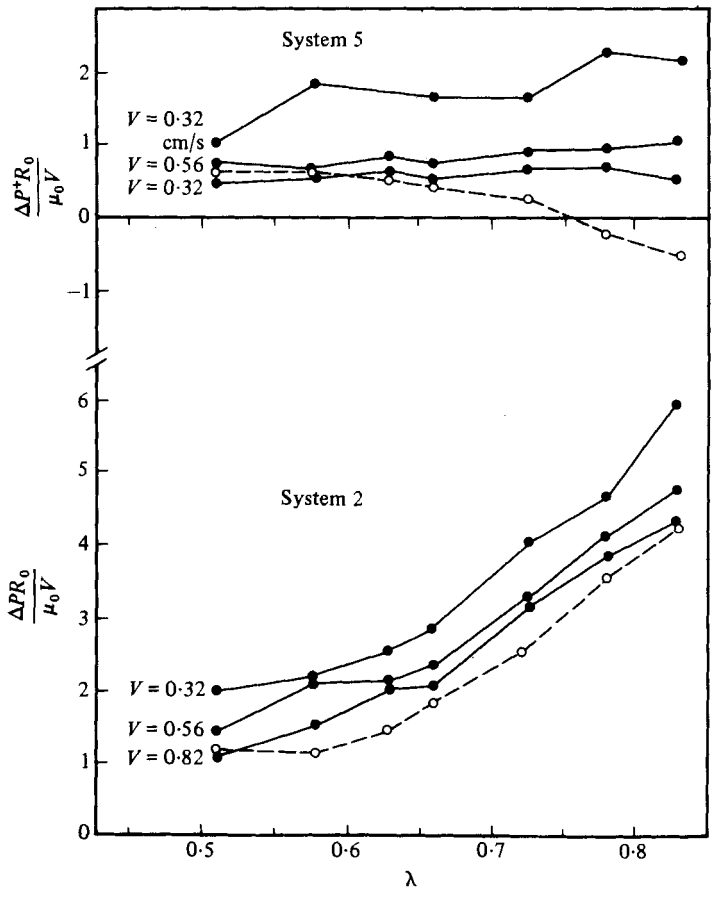


FIGURE 11. Data for dimensionless pressure drop as a function of drop size. ●, systems 2 and 5 (Newtonian). ○, predicted values from (2). Note that the predicted value does not vary with flow rate.

comparison of the theoretical equation (2) with the data. The dependence of $\Delta P^+$ on $\lambda$ for selected Newtonian systems is shown in figure 11. For viscous drops, agreement between data and theory is good, with the values for $\Delta P^+$ from the data exceeding the value given by (2) by 50 % at most. The deviation is smaller for small values of $\lambda$, which is to be expected since the theory is strictly valid only in the small-$\lambda$ limit.

Agreement between data and theory is not as good for low-viscosity drops because the eccentricity term, which unrealistically neglects the effect of the wall, is relatively more important for low values of $\sigma$ than for highly viscous drops, as indicated in table 4. As a result, the value of $\Delta P^+$ calculated from (2) even has the incorrect sign over the entire range of $\lambda$ for system 4 ($\sigma$ = 0·30). The deviation between theory and experiment increases with $\lambda$, a consequence (presumably) of an increase in the magnitude of the neglected wall interaction. On the other hand, in the small-$\lambda$ region, quantitative agreement is still satisfactory, even for low-viscosity drops.

Dependence of $\Delta P^+ R_0/\mu_0 V$ on $V$ enters only through the effect of $V$ on $\beta$, just as in equation (1) for $U/V$. A comparison shows the predicted variation of $\Delta P^+ R_0/\mu_0 V$

with $V$ is much less than indicated by the data, although (2) at least correctly predicts that the qualitative effect of an increase in $V$ is a lower value for $\Delta P^+$.

Bungay & Brenner (1973*a*) have shown that, if wall effects are taken into account, a higher value of $\Delta P^+$ is obtained for given values of $\lambda$ and $\Delta\rho$, at least for rigid particles. They calculated $\Delta P^+$ for a small, rigid sphere in the presence of the tube wall, using the method of reflections combined with the reciprocal theorem. The result for $\Delta P^+ R_0/\mu_0 V$ shows the coefficient of the $\beta^2\lambda^3$ term to be 226. Now, as the authors point out, if (2) is used in the limits $\beta \to 1$, $\sigma \to \infty$, the coefficient of the eccentricity $O(\lambda^3)$ term is only $\frac{160}{3}$, less than one-fourth of the value if wall interaction is included. The data for $\Delta P^+$ for drops in the present experiment generally lie above the value from (2), but below the near-wall prediction for rigid particles. No theoretical result for wall effects on fluid drops is available at the present time.

## 6. Conclusions

Data from a study of the creeping motion of non-neutrally buoyant drops in a horizontal tube have been presented. The measured quantities were the additional pressure difference, the velocity of the drop, the shape, and the gap width between the drop and the wall. These were measured as functions of the material and flow parameters, including drop viscosity, drop density, the size of the drop, the flow rate, and the suspending-fluid rheology.

A major purpose of the study was to identify the effects of variations in the lateral position of the drop, and this was accomplished through variations in the density of the drop fluid. Even small density differences ($\Delta\rho/\rho_0 = 0{\cdot}02$) produced qualitative differences in the dependence of the measured quantities on some variables. For example, eccentrically located particles showed a maximum mobility for an intermediate drop size which is not observed for concentric particles.

The effect of the eccentric position of the drop was to increase the pressure difference over the value for the concentric case. A simultaneous decrease in the relative velocity of the drop was also noted. The dependence of $\Delta P^+$ and $U/V$ on $\Delta\rho/\rho_0$ for large drops decreased as $\Delta\rho/\rho_0$ was made larger. Thus, it appears that although small density differences can make significant changes in the measured values for the quantities studied here, large density differences do not produce correspondingly large deviations from the neutrally buoyant results. Indeed, asymptotic behaviour will be attained at lower values of $\Delta\rho/\rho_0$ as the size of the drop is made larger. The results of this study seem to indicate that small density differences should definitely be considered in the motion of particles in porous-media flow or other related problems, since most practical conditions will probably involve non-neutrally buoyant suspensions. However, above minimal values for $\Delta\rho/\rho_0$, further non-neutral buoyancy can safely be neglected.

The viscoelasticity of the suspending fluid was an important factor in the determination of the shape of the drops as well as the equilibrium lateral position assumed by the drops during flow. There were corresponding changes in $\Delta P^+$ and $U/V$ from the Newtonian case. Since the combination of increased viscosity and normal-stress effects in the viscoelastic fluid provides a mechanism that tends to 'move' particles further away from the wall, the effects of increased density differences were felt at larger values of $\Delta\rho/\rho_0$ than for the corresponding Newtonian case. Thus, the 'asymp-

totic regime' mentioned above will apparently occur at larger values of $\Delta\rho/\rho_0$ for viscoelastic suspending fluids.

For the Newtonian systems, qualitative agreement was generally found between the data and available small-$\lambda$ theoretical expressions that take into account the eccentric position of the drop. For large values of $\lambda$, the effect of drop-fluid viscosity is crucial to the value of $\Delta P^+$, and, therefore, theoretical derivations for solid particles based on lubrication theory are only of use in estimating the additional pressure difference for very viscous drops. However, the mobility of the drop is much less dependent on the drop viscosity and it was shown that lubrication theory can be used to correlate the mobility data. Furthermore, it was found that if a power-law model was used to account for the shear-thinning of the viscoelastic suspending fluid, data for $\Delta P^+$ for large viscous drops could be correlated with results from lubrication theory.

This work was supported by a grant from the National Science Foundation. The authors wish to thank Chris Bockenstette for her assistance in carrying out some of the experiments.

## REFERENCES

BRENNER, H. 1970 Pressure drop due to the motion of neutrally buoyant particles in duct flows. *J. Fluid Mech.* **43**, 641.

BRENNER, H. 1973 Pressure drop due to the motion of neutrally buoyant particles in duct flows. III. Non-neutrally buoyant spherical droplets and bubbles. *Z. angew. Math. Mech.* **53**, 187.

BUNGAY, P. M. & BRENNER, H. 1973 The motion of a closely-fitting sphere in a fluid-filled tube. *Int. J. Multiphase Flow* **1**, 25.

CHAN, P. C.-H. & LEAL, L. G. 1979 The motion of a deformable drop in a second-order fluid. *J. Fluid Mech.* **92**, 131.

DEIBER, J. A. & SCHOWALTER, W. R. 1979 Flow through tubes with sinusoidal axial variations in diameter. *A.I.Ch.E. J.* **25**, 638.

FEDKIW, P. & NEWMAN, J. 1977 Mass transfer at high Péclet numbers for creeping flow in a packed-bed reactor. *A.I.Ch.E. J.* **23**, 255.

FITZ-GERALD, J. M. 1969 Mechanics of red-cell motion through very narrow capillaries. *Proc. R. Soc. Lond.* B **174**, 193.

GOLDSMITH, H. L. & MASON, S. G. 1963 The flow of suspensions through tubes. II. Single large bubbles. *J. Colloid Interface Sci.* **18**, 237.

HETSRONI, G., HABER, S. & WACHOLDER, E. 1970 The flow field in and around a droplet moving axially within a tube. *J. Fluid Mech.* **41**, 689.

HO, B. P. & LEAL, L. G. 1975 The creeping motion of liquid drops through a circular tube of comparable diameter. *J. Fluid Mech.* **71**, 361.

HOCHMUTH, R. M. & SUTERA, S. P. 1970 Spherical caps in low-Reynolds-number tube flow. *Chem. Engng Sci.* **25**, 593.

HOCHMUTH, R. M., MARPLE, R. N. & SUTERA, S. P. 1970 Capillary blood flow. I. Erythrocyte deformation in glass capillaries. *Microvasc. Res.* **2**, 409.

HUPPLER, J. P., ASHARE, E. & HOLMES, L. A. 1967*a* Rheological properties of three solutions. I. Non-Newtonian viscosity, normal stresses, and complex viscosity. *Trans. Soc. Rheol.* **11**, 159.

HUPPLER, J. P., MACDONALD, I. F., ASHARE, E., SPRIGGS, T. W., BIRD, R. B. & HOLMES, L. A. 1967*b* Rheological properties of three solutions. II. Relaxation and growth of shear and normal stresses. *Trans. Soc. Rheol.* **11**, 181.

HYMAN, W. A. & SKALAK, R. 1972*a* Viscous flow of a suspension of liquid drops in a cylindrical tube. *Appl. Sci. Res.* **26**, 27.

HYMAN, W. A. & SKALAK, R. 1972*b* Non-Newtonian behavior of a suspension of liquid drops in tube flow. *A.I.Ch.E. J.* **18**, 149.

LEAL, L. G., SKOOG, J. & ACRIVOS, A. 1971 On the motion of gas bubbles in a viscoelastic fluid. *Can. J. Chem. Engng* **49**, 569.

LIGHTHILL, M. J. 1968 Pressure-forcing of tightly fitting pellets along fluid-filled elastic tubes. *J. Fluid Mech.* **34**, 113.

MARSHALL, R. J. & METZNER, A. B. 1967 Flow of viscoelastic fluids through porous media. *Ind. Engng Chem. Fund.* **6**, 393.

NEIRA, M. A. & PAYATAKES, A. C. 1979 Collocation solution of creeping Newtonian flow through sinusoidal tubes. *A.I.Ch.E. J.* **25**, 725.

OLBRICHT, W. L. 1980 Ph.D. thesis, California Institute of Technology.

OLBRICHT, W. L. & LEAL, L. G. 1981 The creeping flow of immiscible drops through a converging/diverging tube. (In press.)

PAYATAKES, A. C. & NEIRA, M. 1977 Model of the constricted unit cell type for isotropic granular porous media. *A.I.Ch.E. J.* **23**, 922.

PROTHERO, J. & BURTON, A. C. 1961*a* The physics of blood flow in capillaries. I. The nature of the motion. *Biophys. J.* **2**, 199.

PROTHERO, J. & BURTON, A. C. 1961*b* The physics of blood flow in capillaries. III. The pressure required to deform erythrocytes in acid-citrate-dextrose. *Biophys. J.* **2**, 213.

SESHARDI, V., HOCHMUTH, R. M., CROCE, P. A. & SUTERA, S. P. 1970 Capillary blood flow. III. Deformable model cells compared to erythrocytes in vitro. *Microvasc. Res.* **2**, 434.

SIGLI, D. & COUTANCEAU, M. 1977 Effect of finite boundaries on the slow laminar isothermal flow of a viscoelastic liquid around a spherical obstacle. *J. Non-Newt. Fluid Mech.* **2**, 1.

SUTERA, S. P., SESHARDI, V., CROCE, P. A. & HOCHMUTH, R. M. 1970 Capillary blood flow. II. Deformable model cells in tube flow. *Microvasc. Res.* **2**, 420.

TAYLOR, G. I. 1932 The intrinsic viscosity of a fluid containing small drops of another fluid. *Proc. R. Soc. Lond.* A **138**, 41.

TOZEREN, H. & SKALAK, R. 1978 The steady flow of closely fitting incompressible elastic spheres in a tub[illegible]. *Fluid Mech.* **87**, 1.